

Dynamics of a Model of Polluted Lakes via Fractal-Fractional Operators with Two Different Numerical Algorithms

Tanzeela Kanwal^{1,*} Azhar Hussain^{1,2} İbrahim Avci³ Sina Etemad^{4,5}
 Shahram Rezapour^{4,6,7,*} Delfim F. M. Torres^{8,*}

¹Department of Mathematics, University of Sargodha, Sargodha 40100, Pakistan;
 tanzeelakanwal16@gmail.com (T.K.)

²Department of Mathematics, University of Chakwal, Chakwal 48800, Pakistan;
 azhar.hussain@uoc.edu.pk (A.H.)

³Department of Computer Engineering, Faculty of Engineering, Final International University, Kyrenia, Northern Cyprus, via Mersin 10, Turkey;
 ibrahim.avci@final.edu.tr (İ.A.)

⁴Department of Mathematics, Azarbaijan Shahid Madani University, Tabriz, Iran;
 sina.etemad@azaruniv.ac.ir (S.E.); sh.rezapour@azaruniv.ac.ir (S.R.)

⁵Mathematics in Applied Sciences and Engineering Research Group,
 Scientific Research Center, Al-Ayen University, Nasiriyah 64001, Iraq

⁶Department of Mathematics, Kyung Hee University, 26 Kyungheedaero,
 Dongdaemun-gu, Seoul, Republic of Korea

⁷Department of Medical Research, China Medical University Hospital, China
 Medical University, Taichung, Taiwan

⁸Center for Research and Development in Mathematics and Applications (CIDMA), Department of Mathematics, University of Aveiro, 3810-193 Aveiro, Portugal; delfim@ua.pt (D.F.M.T.)

Abstract

We employ Mittag–Leffler type kernels to solve a system of fractional differential equations using fractal-fractional (FF) operators with two fractal and fractional orders. Using the notion of FF-derivatives with nonsingular and nonlocal fading memory, a model of three polluted lakes with one source of pollution is investigated. The properties of a non-decreasing and compact mapping are used in order to prove the existence of a solution for the FF-model of polluted lake system. For this purpose, the Leray–Schauder theorem is used. After exploring stability requirements in four versions, the proposed model of polluted lakes system is then simulated using two new numerical techniques based on Adams–Bashforth and Newton polynomials methods. The effect of fractal-fractional differentiation is illustrated numerically. Moreover, the effect of the FF-derivatives is shown under three specific input models of the pollutant: linear, exponentially decaying, and periodic.

Keywords: Pollution of waters; Fractal-fractional derivatives model; Existence, unicity and stability; Adams–Bashforth and Newton polynomials methods.

MSC: 34A08; 65P99.

*This is a preprint of a paper whose final and definite form is published Open Access in *Chaos Solitons Fractals* at [<https://doi.org/10.1016/j.chaos.2024.114653>].

*Correspondence: tanzeelakanwal16@gmail.com (T.K.); sh.rezapour@azaruniv.ac.ir (S.R.); delfim@ua.pt (D.F.M.T.)

1 Introduction

In the last century, pollution of waters has become a severe danger to the world we live in. The first step in preparing to conserve the natural environment is to monitor pollution levels. Monitoring pollution is possible to achieve with the use of mathematical analysis. Differential equations may be used to simulate environmental contamination, just as they can be used in many other fields. For example, Biazar *et al.* utilized in 2006 a set of differential equations to predict the pollution level in a series of lakes [1]. In concrete, they have proposed a model of triple lakes connected by channels through compartment modeling. Some other scholars have investigated this concept using various methodologies. Yüzbaşı *et al.* [2] analyzed such levels of pollution under the collocation method in 2012. Later, Benhammouda *et al.* [3] utilized another method to solve the pollution model via a modified differential transform. Khader *et al.* [4] have also created a fractional case model and used the matrix properties in 2013. Recently, in 2019, Bildik and Deniz [5] considered an Atangana–Baleanu based model for approximating the solutions of a polluted lake system. After that, Ahmed and Khan turned to a similar model of lake pollution via different fractional methods [6]. In 2020, Prakasha and Veerasha [7] solved such a system of polluted lakes via the so-called q-HATM method. More recently, in 2022, Shiri and Baleanu have done a research on the amount of pollution in a three-compartmental model and derived some analytical results [8]. During these years, fractional models of real-world processes have been studied by many other researchers, showing the applicability of fractional operators in mathematical modeling: see, e.g., [9, 10, 11, 12, 13, 14, 15]. Here we propose and study a mathematical model via a generalized family of derivatives equipped with two parameters.

Atangana introduced a new class of fractal-fractional notions, which brings together the two applicable areas of fractal and fractional calculi [16]. The structure of these operators is a convolution of the power-law, exponential law, and modified Mittag–Leffler law with fractal derivatives, which establishes a connection between fractional and fractal mathematics. The fractal dimension and order are the two components of these operators and differential equations with fractal-fractional derivatives convert the putative system’s order and dimension into a rational system. Because of this characteristic, conventional differential equations are naturally extended to systems with any order of derivatives and dimensions. The goal of these coupled operators is to look at distinct nonlocal boundary value problems (BVPs) or initial value problems (IVPs) that have fractal tendencies in nature. Many scholars provided results and discoveries in this area, demonstrating that fractal-fractional operators are more effective at describing real-world data and for mathematical modeling. Examples of such mathematical models include: fractal-fractional structures of dynamics of corona viruses [17], malaria transmission [18], dynamics of COVID-19 in Wuhan [19], transmission of AH1N1/09 virus [20], dynamics of Q fever [21], HIV [22], dynamics of CD4⁺ cells [23], tuberculosis disease [24], etc.

The incorporation of fractal-fractional (FF) operators with dual fractal and fractional orders in scientific research presents a promising avenue with multifaceted advantages. By leveraging two orders simultaneously, this approach allows for a more nuanced and refined representation of complex systems, capturing intricate patterns and irregularities that traditional methods might overlook. The synergy of fractal geometry and fractional calculus enhances the modeling and analysis of real-world phenomena, providing a more accurate reflection of the inherent self-similar structures and non-integer order dynamics. This not only refines our understanding of intricate processes but also facilitates the development of more robust mathematical models that can be applied across various disciplines. The utilization of FF operators holds the potential to revolutionize fields ranging from signal processing to image analysis, offering a versatile toolkit to address challenges that demand a deeper comprehension of intricate, multifractal behaviors. Embracing this innovative paradigm contributes to a more holistic and precise approach in scientific investigations, opening new frontiers for exploration and discovery. Here we conduct an analysis of a fractal-fractional model of polluted lakes in terms of various different characteristics.

The paper is organized as follows. In Section 2, we introduce a fractal-fractional system to model polluted lakes. Existence of a solution to the proposed system is proved in Section 3 by using the Leray–Schauder theorem. In Section 4, we employ the Banach principle for contrac-

tions to demonstrate uniqueness of solution. Furthermore, using functional analysis, numerous requirements for different types of stability for the solution to the polluted lakes system model are explored in Section 5. To simulate our model, we use two different techniques: a fractional Adams–Bashforth approach (Section 6) and a second one based on Newton’s polynomials (Section 7). The obtained theoretical results are then tested in Section 8 by applying our algorithms with some concrete data under various fractal and fractional order values in three different cases: linear, exponentially decaying and periodic input real models. We end with Section 9 of conclusion.

2 The FF-model for a polluted system of three lakes

We model three lakes. Using three lakes in a system might be a good practical choice based on various factors such as land availability, cost, and efficiency. The decision of considering here three lakes is not purely mathematical, but involves environmental, economic, and logistical considerations. Mathematical modeling could help optimize the distribution and size of the lakes, but it is essential to balance these factors for a sustainable and effective solution. Therefore, we restrict ourselves to three lakes and their channels with a pollutant source. One can generalize our results to a finite number of lakes.

Each lake is treated as a compartment, a linking channel between two lakes being viewed as a pipe connecting the compartments. The direction of the flow across each channel or pipeline is shown by arrows. A contaminant c is considered in the first lake. By $c(s)$ we denote the rate at which the contaminant/pollutant enters Lake 1 at time s . The major purpose is to determine the pollution levels in each lake at any given moment. To do so, we regard the concentration $C_i(s)$ of the pollutant in the lake i at time s , $s \geq 0$, by

$$C_i(s) = \frac{L_i(s)}{V_i}, \quad (1)$$

where V_i denotes the water volume at lake i , $i \in \{1, 2, 3\}$, assumed to be constant, and $L_i(s)$ specifies the quantity of pollution that is equally distributed over each lake at time s . We are interested to model the situation shown in Figure 1, where we use the symbol F_{ji} to represent the flow rate entering the j th lake from the i th. Based on Figure 1, we derive the following conditions:

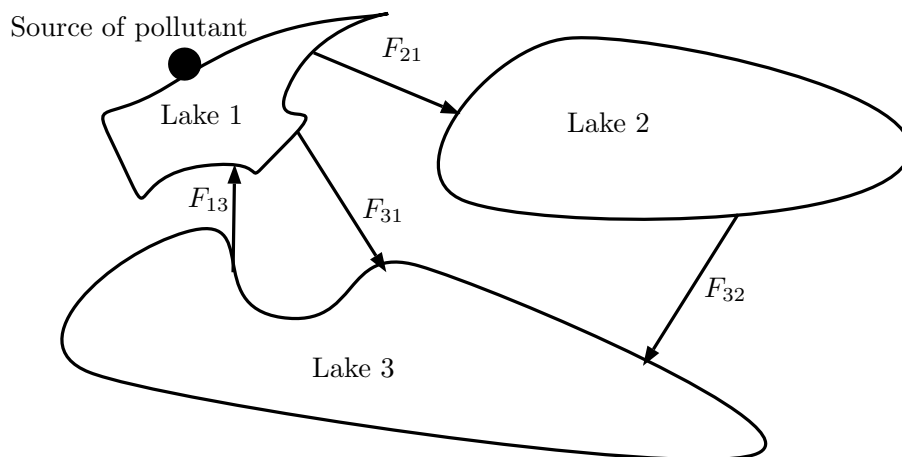


Figure 1: Schematic of channels interconnecting the three lakes being modeled.

$$\begin{aligned} \text{Lake 1 : } & F_{13} = F_{31} + F_{21}, \\ \text{Lake 2 : } & F_{21} = F_{32}, \\ \text{Lake 3 : } & F_{32} + F_{31} = F_{13}. \end{aligned} \quad (2)$$

Note that $F_{12} = 0$ since there exists no pipe between the second and the first lakes. The flux $\mathcal{F}_{ji}(s)$ of pollutant flowing from the i th lake to the j th lake at an arbitrary time s measures the flow rate of the concentration of pollutant. This index equals

$$\mathcal{F}_{ji}(s) = F_{ji}C_i(s) = F_{ji}\frac{L_i(s)}{V_i}. \quad (3)$$

Based on the principle that the rate of change of the pollutant is given by the difference between the input rate and the output rate, we propose here the following fractal-fractional model for the dynamic behavior of the polluted lake system of three lakes via the generalized Mittag–Leffler kernel:

$$\begin{cases} \mathbf{FFML}\mathcal{D}_{0,s}^{(\theta,\sigma)}L_1(s) = \frac{F_{13}}{V_3}L_3(s) + c(s) - \frac{F_{31}}{V_1}L_1(s) - \frac{F_{21}}{V_1}L_1(s), \\ \mathbf{FFML}\mathcal{D}_{0,s}^{(\theta,\sigma)}L_2(s) = \frac{F_{21}}{V_1}L_1(s) - \frac{F_{32}}{V_2}L_2(s), \\ \mathbf{FFML}\mathcal{D}_{0,s}^{(\theta,\sigma)}L_3(s) = \frac{F_{31}}{V_1}L_1(s) + \frac{F_{32}}{V_2}L_2(s) - \frac{F_{13}}{V_3}L_3(s), \end{cases} \quad (4)$$

subject to

$$L_1(0) = L_{1,0} \geq 0, \quad L_2(0) = L_{2,0} \geq 0, \quad L_3(0) = L_{3,0} \geq 0, \quad (5)$$

where $\mathbf{FFML}\mathcal{D}_{0,s}^{(\theta,\sigma)}$ is the (θ, σ) -fractal-fractional derivative with Mittag–Leffler type kernel of fractional and fractal orders $\theta \in (0, 1]$ and $\sigma \in (0, 1]$, respectively, as introduced by Atangana in [16].

Definition 1 (See [16]). *Let $f : (a, b) \rightarrow [0, \infty)$ be a continuous map that is fractal differentiable of dimension σ . In this case, the Riemann–Liouville (θ, σ) -fractal-fractional derivative of f with the generalized Mittag–Leffler type kernel of order θ is given by*

$$\mathbf{FFML}\mathcal{D}_{a,s}^{(\theta,\sigma)}f(s) = \frac{\mathcal{AB}(\theta)}{1-\theta} \frac{d}{ds^\sigma} \int_a^s \mathbb{E}_\theta \left[-\frac{\theta}{1-\theta}(s-\mathfrak{w})^\theta \right] f(\mathfrak{w}) d\mathfrak{w}, \quad 0 < \theta, \sigma \leq 1, \quad (6)$$

where

$$\frac{df(\mathfrak{w})}{d\mathfrak{w}^\sigma} = \lim_{s \rightarrow \mathfrak{w}} \frac{f(s) - f(\mathfrak{w})}{s^\sigma - \mathfrak{w}^\sigma}$$

is the fractal derivative and $\mathcal{AB}(\theta) = 1 - \theta + \frac{\theta}{\Gamma(\theta)}$ with $\mathcal{AB}(0) = \mathcal{AB}(1) = 1$.

In what follows, we also use the corresponding notion of fractal-fractional integral.

Definition 2 (See [16]). *The (θ, σ) -fractal-fractional integral of a function f with generalized kernel is given by*

$$\mathbf{FFML}\mathcal{I}_{a,s}^{(\theta,\sigma)}f(s) = \frac{\theta\sigma}{\mathcal{AB}(\theta)\Gamma(\theta)} \int_a^s \mathfrak{w}^{\sigma-1}(s-\mathfrak{w})^{\theta-1}f(\mathfrak{w})d\mathfrak{w} + \frac{(1-\theta)\sigma s^{\sigma-1}}{\mathcal{AB}(\theta)}f(s), \quad (7)$$

if it exists, where $\theta, \sigma > 0$.

3 Existence

We begin by proving existence of solution to our problem (4)–(5). For that we use fixed point theory. To conduct our qualitative analysis, let us define the Banach space $\mathbb{X} = \mathbb{C}^3$, where $\mathbb{C} = C(\mathbb{J}, \mathbb{R})$ with

$$\|\mathbb{K}\|_{\mathbb{X}} = \|(L_1, L_2, L_3)\|_{\mathbb{X}} = \max \{|W(s)| : s \in \mathbb{J}\},$$

for $|W| := |L_1| + |L_2| + |L_3|$. We rewrite the right-hand-side of the fractal-fractional polluted lake system (4) as

$$\begin{cases} \mathbb{Q}_1(s, L_1(s), L_2(s), L_3(s)) = \frac{F_{13}}{V_3} L_3(s) + c(s) - \frac{F_{31}}{V_1} L_1(s) - \frac{F_{21}}{V_1} L_1(s), \\ \mathbb{Q}_2(s, L_1(s), L_2(s), L_3(s)) = \frac{F_{21}}{V_1} L_1(s) - \frac{F_{32}}{V_2} L_2(s), \\ \mathbb{Q}_3(s, L_1(s), L_2(s), L_3(s)) = \frac{F_{31}}{V_1} L_1(s) + \frac{F_{32}}{V_2} L_2(s) - \frac{F_{13}}{V_3} L_3(s). \end{cases} \quad (8)$$

In this case, the fractal-fractional polluted lake system (4) is transformed into the following system:

$$\begin{cases} \mathbf{ABR}\mathcal{D}_{0,s}^\theta L_1(s) = \sigma s^{\sigma-1} \mathbb{Q}_1(s, L_1(s), L_2(s), L_3(s)), \\ \mathbf{ABR}\mathcal{D}_{0,s}^\theta L_2(s) = \sigma s^{\sigma-1} \mathbb{Q}_2(s, L_1(s), L_2(s), L_3(s)), \\ \mathbf{ABR}\mathcal{D}_{0,s}^\theta L_3(s) = \sigma s^{\sigma-1} \mathbb{Q}_3(s, L_1(s), L_2(s), L_3(s)). \end{cases} \quad (9)$$

In view of (9), we rewrite our tree-state system as the compact IVP

$$\begin{cases} \mathbf{ABR}\mathcal{D}_{0,s}^\theta \mathbb{K}(s) = \sigma s^{\sigma-1} \mathbb{Q}(s, \mathbb{K}(s)), \\ \mathbb{K}(0) = \mathbb{K}_0, \end{cases} \quad (10)$$

where

$$\mathbb{K}(s) = (L_1(s), L_2(s), L_3(s))^T, \quad \mathbb{K}_0 = (L_{1,0}, L_{2,0}, L_{3,0})^T, \quad \theta, \sigma \in (0, 1], \quad (11)$$

and

$$\mathbb{Q}(s, \mathbb{K}(s)) = \begin{cases} \mathbb{Q}_1(s, L_1(s), L_2(s), L_3(s)), \\ \mathbb{Q}_2(s, L_1(s), L_2(s), L_3(s)), \\ \mathbb{Q}_3(s, L_1(s), L_2(s), L_3(s)), \quad s \in \mathbb{J}. \end{cases} \quad (12)$$

By definition and by (10), we have

$$\frac{\mathcal{AB}(\theta)}{1-\theta} \frac{d}{ds} \int_0^s \mathbb{E}_\theta \left[-\frac{\theta}{1-\theta} (s-\mathfrak{w})^\theta \right] \mathbb{K}(\mathfrak{w}) d\mathfrak{w} = \sigma s^{\sigma-1} \mathbb{Q}(s, \mathbb{K}(s)). \quad (13)$$

Applying the fractal-fractional Atangana–Baleanu integral on (13), we get

$$\mathbb{K}(s) = \mathbb{K}(0) + \frac{\theta\sigma}{\mathcal{AB}(\theta)\Gamma(\theta)} \int_0^s \mathfrak{w}^{\sigma-1} (s-\mathfrak{w})^{\theta-1} \mathbb{Q}(\mathfrak{w}, \mathbb{K}(\mathfrak{w})) d\mathfrak{w} + \frac{(1-\theta)\sigma s^{\sigma-1}}{\mathcal{AB}(\theta)} \mathbb{Q}(s, \mathbb{K}(s)). \quad (14)$$

The extended representation of (14) is given by

$$\begin{cases} L_1(s) = L_{1,0} + \frac{(1-\theta)\sigma s^{\sigma-1}}{\mathcal{AB}(\theta)} \mathbb{Q}_1(s, L_1(s), L_2(s), L_3(s)) \\ \quad + \frac{\theta\sigma}{\mathcal{AB}(\theta)\Gamma(\theta)} \int_0^s \mathfrak{w}^{\sigma-1} (s-\mathfrak{w})^{\theta-1} \mathbb{Q}_1(\mathfrak{w}, L_1(\mathfrak{w}), L_2(\mathfrak{w}), L_3(\mathfrak{w})) d\mathfrak{w}, \\ L_2(s) = L_{2,0} + \frac{(1-\theta)\sigma s^{\sigma-1}}{\mathcal{AB}(\theta)} \mathbb{Q}_2(s, L_1(s), L_2(s), L_3(s)) \\ \quad + \frac{\theta\sigma}{\mathcal{AB}(\theta)\Gamma(\theta)} \int_0^s \mathfrak{w}^{\sigma-1} (s-\mathfrak{w})^{\theta-1} \mathbb{Q}_2(\mathfrak{w}, L_1(\mathfrak{w}), L_2(\mathfrak{w}), L_3(\mathfrak{w})) d\mathfrak{w}, \\ L_3(s) = L_{3,0} + \frac{(1-\theta)\sigma s^{\sigma-1}}{\mathcal{AB}(\theta)} \mathbb{Q}_3(s, L_1(s), L_2(s), L_3(s)) \\ \quad + \frac{\theta\sigma}{\mathcal{AB}(\theta)\Gamma(\theta)} \int_0^s \mathfrak{w}^{\sigma-1} (s-\mathfrak{w})^{\theta-1} \mathbb{Q}_3(\mathfrak{w}, L_1(\mathfrak{w}), L_2(\mathfrak{w}), L_3(\mathfrak{w})) d\mathfrak{w}. \end{cases} \quad (15)$$

To derive a fixed-point problem, we now define the self-map $F : \mathbb{X} \rightarrow \mathbb{X}$ as

$$F(\mathbb{K}(s)) = \mathbb{K}(0) + \frac{(1-\theta)\sigma s^{\sigma-1}}{\mathcal{AB}(\theta)} \mathbb{Q}(s, \mathbb{K}(s)) + \frac{\theta\sigma}{\mathcal{AB}(\theta)\Gamma(\theta)} \int_0^s \mathfrak{w}^{\sigma-1} (s-\mathfrak{w})^{\theta-1} \mathbb{Q}(\mathfrak{w}, \mathbb{K}(\mathfrak{w})) \, d\mathfrak{w}. \quad (16)$$

To prove existence of solution to our fractal-fractional polluted lake system (4), we make use of the following Leray–Schauder theorem.

Theorem 3 (Leray–Schauder fixed point theorem [25]). *Let \mathbb{X} be a Banach space, $\mathbb{E} \subset \mathbb{X}$ a closed convex and bounded set, and $\mathbb{O} \subset \mathbb{E}$ an open set with $0 \in \mathbb{O}$. Then, under the compact and continuous mapping $F : \mathbb{O} \rightarrow \mathbb{E}$, either:*

(Y1) $\exists y \in \bar{\mathbb{O}}$ s.t. $y = F(y)$, or

(Y2) $\exists y \in \partial\mathbb{O}$, $\mu \in (0, 1)$ such that $y = \mu F(y)$.

Given that the polluted lake system models a real-world problem, its existence is subject to certain constraints. These constraints, denoted in Theorem 4 as (P1) and (P2), play a crucial role in shaping the dynamics and characteristics of the system. Indeed, (P1) and (P2) are indispensable to define and regulate the behavior of the polluted lake system within the confines of practicality and reality. Recognizing these constraints is essential for constructing a comprehensive understanding of the system and developing effective strategies.

Theorem 4. *Let $\mathbb{Q} \in C(\mathbb{J} \times \mathbb{X}, \mathbb{X})$. If*

(P1) $\exists \varphi \in L^1(\mathbb{J}, \mathbb{R}^+)$ and $\exists A \in C([0, \infty), (0, \infty))$ (A non-decreasing) such that $\forall s \in \mathbb{J}$ and $\mathbb{K} \in \mathbb{X}$,

$$|\mathbb{Q}(s, \mathbb{K}(s))| \leq \varphi(s)A(|\mathbb{K}(s)|);$$

(P2) $\exists \omega > 0$ such that

$$\frac{\omega}{\mathbb{K}_0 + \left[\frac{(1-\theta)\sigma S^{\sigma-1}}{\mathcal{AB}(\theta)} + \frac{\theta\sigma S^{\theta+\sigma-1}\Gamma(\sigma)}{\mathcal{AB}(\theta)\Gamma(\theta+\sigma)} \right] \varphi_0^* A(\omega)} > 1 \quad (17)$$

with $\varphi_0^* = \sup_{s \in \mathbb{J}} |\varphi(s)|$;

then there exists a solution to the fractal-fractional polluted lake system (4).

Proof. First, consider $F : \mathbb{X} \rightarrow \mathbb{X}$, which is formulated in (16), and assume

$$N_r = \left\{ \mathbb{K} \in \mathbb{X} : \|\mathbb{K}\|_{\mathbb{X}} \leq r \right\},$$

for some $r > 0$. Clearly, as \mathbb{Q} is continuous, thus F is also so. From (P1), we get

$$\begin{aligned} |F(\mathbb{K}(s))| &\leq |\mathbb{K}(0)| + \frac{(1-\theta)\sigma s^{\sigma-1}}{\mathcal{AB}(\theta)} |\mathbb{Q}(s, \mathbb{K}(s))| \\ &\quad + \frac{\theta\sigma}{\mathcal{AB}(\theta)\Gamma(\theta)} \int_0^s \mathfrak{w}^{\sigma-1} (s-\mathfrak{w})^{\theta-1} |\mathbb{Q}(\mathfrak{w}, \mathbb{K}(\mathfrak{w}))| \, d\mathfrak{w} \\ &\leq \mathbb{K}_0 + \frac{(1-\theta)\sigma s^{\sigma-1}}{\mathcal{AB}(\theta)} \varphi(s)A(|\mathbb{K}(s)|) \\ &\quad + \frac{\theta\sigma}{\mathcal{AB}(\theta)\Gamma(\theta)} \int_0^s \mathfrak{w}^{\sigma-1} (s-\mathfrak{w})^{\theta-1} \varphi(\mathfrak{w})A(|\mathbb{K}(\mathfrak{w})|) \, d\mathfrak{w} \end{aligned}$$

$$\begin{aligned}
 &\leq \mathbb{K}_0 + \frac{(1-\theta)\sigma S^{\sigma-1}}{\mathcal{AB}(\theta)} \varphi_0^* A(r) + \frac{\theta\sigma S^{\theta+\sigma-1} B(\theta, \sigma)}{\mathcal{AB}(\theta)\Gamma(\theta)} \varphi_0^* A(r) \\
 &= \mathbb{K}_0 + \frac{(1-\theta)\sigma S^{\sigma-1}}{\mathcal{AB}(\theta)} \varphi_0^* A(r) + \frac{\theta\sigma S^{\theta+\sigma-1} \Gamma(\sigma)}{\mathcal{AB}(\theta)\Gamma(\theta+\sigma)} \varphi_0^* A(r),
 \end{aligned}$$

for $\mathbb{K} \in N_r$. Hence,

$$\|F\mathbb{K}\|_{\mathbb{X}} \leq \mathbb{K}_0 + \left[\frac{(1-\theta)\sigma S^{\sigma-1}}{\mathcal{AB}(\theta)} + \frac{\theta\sigma S^{\theta+\sigma-1} \Gamma(\sigma)}{\mathcal{AB}(\theta)\Gamma(\theta+\sigma)} \right] \varphi_0^* A(r) < \infty. \quad (18)$$

Thus, F is uniformly bounded on \mathbb{X} . Now, take $s, v \in [0, S]$ such that $s < v$ and $\mathbb{K} \in N_r$. By denoting

$$\sup_{(s, \mathbb{K}) \in \mathbb{J} \times N_r} |\mathbb{Q}(s, \mathbb{K}(s))| = \mathbb{Q}^* < \infty,$$

we estimate

$$\begin{aligned}
 |F(\mathbb{K}(v)) - F(\mathbb{K}(s))| &\leq \left| \frac{(1-\theta)\sigma v^{\sigma-1}}{\mathcal{AB}(\theta)} \mathbb{Q}(v, \mathbb{K}(v)) - \frac{(1-\theta)\sigma s^{\sigma-1}}{\mathcal{AB}(\theta)} \mathbb{Q}(s, \mathbb{K}(s)) \right. \\
 &\quad + \frac{\theta\sigma}{\mathcal{AB}(\theta)\Gamma(\theta)} \int_0^v \mathfrak{w}^{\sigma-1} (v-\mathfrak{w})^{\theta-1} \mathbb{Q}(\mathfrak{w}, \mathbb{K}(\mathfrak{w})) \, d\mathfrak{w} \\
 &\quad \left. - \frac{\theta\sigma}{\mathcal{AB}(\theta)\Gamma(\theta)} \int_0^s \mathfrak{w}^{\sigma-1} (s-\mathfrak{w})^{\theta-1} \mathbb{Q}(\mathfrak{w}, \mathbb{K}(\mathfrak{w})) \, d\mathfrak{w} \right| \\
 &\leq \frac{(1-\theta)\sigma \mathbb{Q}^*}{\mathcal{AB}(\theta)} (v^{\sigma-1} - s^{\sigma-1}) \\
 &\quad + \frac{\theta\sigma \mathbb{Q}^*}{\mathcal{AB}(\theta)\Gamma(\theta)} \left| \int_0^v \mathfrak{w}^{\sigma-1} (v-\mathfrak{w})^{\theta-1} \, d\mathfrak{w} - \int_0^s \mathfrak{w}^{\sigma-1} (s-\mathfrak{w})^{\theta-1} \, d\mathfrak{w} \right| \\
 &\leq \frac{(1-\theta)\sigma \mathbb{Q}^*}{\mathcal{AB}(\theta)} (v^{\sigma-1} - s^{\sigma-1}) + \frac{\theta\sigma \mathbb{Q}^* B(\theta, \sigma)}{\mathcal{AB}(\theta)\Gamma(\theta)} [v^{\theta+\sigma-1} - s^{\theta+\sigma-1}] \\
 &= \frac{(1-\theta)\sigma \mathbb{Q}^*}{\mathcal{AB}(\theta)} (v^{\sigma-1} - s^{\sigma-1}) + \frac{\theta\sigma \mathbb{Q}^* \Gamma(\sigma)}{\mathcal{AB}(\theta)\Gamma(\theta+\sigma)} [v^{\theta+\sigma-1} - s^{\theta+\sigma-1}].
 \end{aligned} \quad (19)$$

We see that the right-hand side of (19) approaches to 0 independent of \mathbb{K} , as $v \rightarrow s$. Consequently,

$$\|F(\mathbb{K}(v)) - F(\mathbb{K}(s))\|_{\mathbb{X}} \rightarrow 0,$$

when $v \rightarrow s$. This gives the equicontinuity of F and, accordingly, the compactness of F on N_r by the Arzelà–Ascoli theorem. As Theorem 3 is fulfilled on F , we have one of (Y1) or (Y2). From (P2), we set

$$\Phi := \left\{ \mathbb{K} \in \mathbb{X} : \|\mathbb{K}\|_{\mathbb{X}} < \omega \right\},$$

for some $\omega > 0$, such that

$$\mathbb{K}_0 + \left[\frac{(1-\theta)\sigma S^{\sigma-1}}{\mathcal{AB}(\theta)} + \frac{\theta\sigma S^{\theta+\sigma-1} \Gamma(\sigma)}{\mathcal{AB}(\theta)\Gamma(\theta+\sigma)} \right] \varphi_0^* A(\omega) < \omega.$$

From (P1) and (18), we have

$$\|F\mathbb{K}\|_{\mathbb{X}} \leq \mathbb{K}_0 + \left[\frac{(1-\theta)\sigma S^{\sigma-1}}{\mathcal{AB}(\theta)} + \frac{\theta\sigma S^{\theta+\sigma-1} \Gamma(\sigma)}{\mathcal{AB}(\theta)\Gamma(\theta+\sigma)} \right] \varphi_0^* A(\|\mathbb{K}\|_{\mathbb{X}}). \quad (20)$$

Suppose that there are $\mathbb{K} \in \partial\Phi$ and $0 < \mu < 1$ such that $\mathbb{K} = \mu F(\mathbb{K})$. Then, by (20), we write

$$\begin{aligned} \omega = \|\mathbb{K}\|_{\mathbb{X}} &= \mu \|F\mathbb{K}\|_{\mathbb{X}} < \mathbb{K}_0 + \left[\frac{(1-\theta)\sigma S^{\sigma-1}}{\mathcal{AB}(\theta)} + \frac{\theta\sigma S^{\theta+\sigma-1}\Gamma(\sigma)}{\mathcal{AB}(\theta)\Gamma(\theta+\sigma)} \right] \varphi_0^* A(\|\mathbb{K}\|_{\mathbb{X}}) \\ &< \mathbb{K}_0 + \left[\frac{(1-\theta)\sigma S^{\sigma-1}}{\mathcal{AB}(\theta)} + \frac{\theta\sigma S^{\theta+\sigma-1}\Gamma(\sigma)}{\mathcal{AB}(\theta)\Gamma(\theta+\sigma)} \right] \varphi_0^* A(\omega) < \omega, \end{aligned}$$

which cannot hold true. Thus, (Y2) is not satisfied and F admits a fixed-point in $\bar{\Phi}$ by Theorem 3. This proves the existence of a solution to the FF polluted lake model (4). \square

4 Uniqueness

As a first step to prove uniqueness of solution to our problem (4)–(5), we begin by investigating a Lipschitz property of the fractal-fractional polluted lake system (4).

Lemma 5. Consider $L_1, L_2, L_3, L_1^*, L_2^*, L_3^* \in \mathbb{C} := C(\mathbb{J}, \mathbb{R})$, and let

(C1) $\|L_1\| \leq \beta_1, \|L_2\| \leq \beta_2, \|L_3\| \leq \beta_3$ for some constants $\beta_1, \beta_2, \beta_3 > 0$.

Then, $\mathbb{Q}_1, \mathbb{Q}_2$, and \mathbb{Q}_3 defined in (8) fulfill the Lipschitz property with constants $\alpha_1, \alpha_2, \alpha_3 > 0$ with respect to the relevant components, where

$$\alpha_1 = \frac{F_{31} + F_{21}}{V_1}, \quad \alpha_2 = \frac{F_{32}}{V_2}, \quad \alpha_3 = \frac{F_{13}}{V_3}. \quad (21)$$

Proof. For \mathbb{Q}_1 , we take $L_1, L_1^* \in \mathbb{C} := C(\mathbb{J}, \mathbb{R})$ arbitrarily, and we have

$$\begin{aligned} &\|\mathbb{Q}_1(s, L_1(s), L_2(s), L_3(s)) - \mathbb{Q}_1(s, L_1^*(s), L_2(s), L_3(s))\| \\ &= \left\| \left(-\frac{F_{31}}{V_1} L_1(s) - \frac{F_{21}}{V_1} L_1(s) \right) - \left(-\frac{F_{31}}{V_1} L_1^*(s) - \frac{F_{21}}{V_1} L_1^*(s) \right) \right\| \\ &\leq \left[\frac{F_{31} + F_{21}}{V_1} \right] \|L_1(s) - L_1^*(s)\| = \alpha_1 \|L_1(s) - L_1^*(s)\|. \end{aligned} \quad (22)$$

From (22), we find out that \mathbb{Q}_1 is Lipschitz with respect to L_1 under the constant $\alpha_1 > 0$. For \mathbb{Q}_2 , we choose arbitrary $L_2, L_2^* \in \mathbb{C} := C(\mathbb{J}, \mathbb{R})$, and estimate

$$\begin{aligned} &\|\mathbb{Q}_2(s, L_1(s), L_2(s), L_3(s)) - \mathbb{Q}_2(s, L_1(s), L_2^*(s), L_3(s))\| \\ &= \left\| \left(-\frac{F_{32}}{V_2} L_2(s) \right) - \left(-\frac{F_{32}}{V_2} L_2^*(s) \right) \right\| \\ &\leq \left[\frac{F_{32}}{V_2} \right] \|L_2(s) - L_2^*(s)\| \\ &= \alpha_2 \|L_2(s) - L_2^*(s)\|. \end{aligned}$$

This means that \mathbb{Q}_2 is Lipschitz with respect to L_2 under the constant $\alpha_2 > 0$. Finally, for arbitrary elements $L_3, L_3^* \in \mathbb{C} := C(\mathbb{J}, \mathbb{R})$, we have

$$\begin{aligned} &\|\mathbb{Q}_3(s, L_1(s), L_2(s), L_3(s)) - \mathbb{Q}_3(s, L_1(s), L_2(s), L_3^*(s))\| \\ &= \left\| \left(-\frac{F_{13}}{V_3} L_3(s) \right) - \left(-\frac{F_{13}}{V_3} L_3^*(s) \right) \right\| \end{aligned}$$

$$\begin{aligned} &\leq \left[\frac{F_{13}}{V_3} \right] \|L_3(s) - L_3^*(s)\| \\ &= \alpha_3 \|L_3(s) - L_3^*(s)\|. \end{aligned}$$

This shows that \mathbb{Q}_3 is Lipschitzian with respect to L_3 with $\alpha_3 > 0$. Therefore, the kernel functions \mathbb{Q}_1 , \mathbb{Q}_2 , and \mathbb{Q}_3 are Lipschitz, respectively with constants $\alpha_1, \alpha_2, \alpha_3 > 0$. \square

By invoking Lemma 5, we now prove uniqueness of solution to the FF-system (4).

Theorem 6. *Let (C1) hold. If*

$$\left[\frac{(1-\theta)\sigma S^{\sigma-1}}{\mathcal{AB}(\theta)} + \frac{\theta\sigma S^{\theta+\sigma-1}\Gamma(\sigma)}{\mathcal{AB}(\theta)\Gamma(\theta+\sigma)} \right] \alpha_j < 1, \quad (23)$$

for $j \in \{1, 2, 3\}$ and where $\alpha_j > 0$ are the Lipschitz constants introduced by (21), then the fractal-fractional polluted lake system (4) possesses exactly one solution.

Proof. We do the proof by contradiction. Assume there exists another solution to the fractal-fractional polluted lake system (4), namely $(L_1^*(s), L_2^*(s), L_3^*(s))$, under initial conditions

$$L_1^*(0) = L_{1,0}, \quad L_2^*(0) = L_{2,0}, \quad L_3^*(0) = L_{3,0}.$$

From (15), we have

$$\begin{aligned} L_1^*(s) &= L_{1,0} + \frac{(1-\theta)\sigma s^{\sigma-1}}{\mathcal{AB}(\theta)} \mathbb{Q}_1(s, L_1^*(s), L_2^*(s), L_3^*(s)) \\ &\quad + \frac{\theta\sigma}{\mathcal{AB}(\theta)\Gamma(\theta)} \int_0^s \mathfrak{w}^{\sigma-1} (s-\mathfrak{w})^{\theta-1} \mathbb{Q}_1(\mathfrak{w}, L_1^*(\mathfrak{w}), L_2^*(\mathfrak{w}), L_3^*(\mathfrak{w})) \, d\mathfrak{w}, \end{aligned}$$

$$\begin{aligned} L_2^*(s) &= L_{2,0} + \frac{(1-\theta)\sigma s^{\sigma-1}}{\mathcal{AB}(\theta)} \mathbb{Q}_2(s, L_1^*(s), L_2^*(s), L_3^*(s)) \\ &\quad + \frac{\theta\sigma}{\mathcal{AB}(\theta)\Gamma(\theta)} \int_0^s \mathfrak{w}^{\sigma-1} (s-\mathfrak{w})^{\theta-1} \mathbb{Q}_2(\mathfrak{w}, L_1^*(\mathfrak{w}), L_2^*(\mathfrak{w}), L_3^*(\mathfrak{w})) \, d\mathfrak{w}, \end{aligned}$$

and

$$\begin{aligned} L_3^*(s) &= L_{3,0} + \frac{(1-\theta)\sigma s^{\sigma-1}}{\mathcal{AB}(\theta)} \mathbb{Q}_3(s, L_1^*(s), L_2^*(s), L_3^*(s)) \\ &\quad + \frac{\theta\sigma}{\mathcal{AB}(\theta)\Gamma(\theta)} \int_0^s \mathfrak{w}^{\sigma-1} (s-\mathfrak{w})^{\theta-1} \mathbb{Q}_3(\mathfrak{w}, L_1^*(\mathfrak{w}), L_2^*(\mathfrak{w}), L_3^*(\mathfrak{w})) \, d\mathfrak{w}. \end{aligned}$$

In this case, we estimate

$$\begin{aligned} |L_1(s) - L_1^*(s)| &\leq \frac{(1-\theta)\sigma s^{\sigma-1}}{\mathcal{AB}(\theta)} \left| \mathbb{Q}_1(s, L_1(s), L_2(s), L_3(s)) - \mathbb{Q}_1(s, L_1^*(s), L_2^*(s), L_3^*(s)) \right| \\ &\quad + \frac{\theta\sigma}{\mathcal{AB}(\theta)\Gamma(\theta)} \int_0^s \mathfrak{w}^{\sigma-1} (s-\mathfrak{w})^{\theta-1} \\ &\quad \times \left| \mathbb{Q}_1(\mathfrak{w}, L_1(\mathfrak{w}), L_2(\mathfrak{w}), L_3(\mathfrak{w})) - \mathbb{Q}_1(\mathfrak{w}, L_1^*(\mathfrak{w}), L_2^*(\mathfrak{w}), L_3^*(\mathfrak{w})) \right| \, d\mathfrak{w} \\ &\leq \frac{(1-\theta)\sigma s^{\sigma-1}}{\mathcal{AB}(\theta)} \alpha_1 \|L_1 - L_1^*\| + \frac{\theta\sigma}{\mathcal{AB}(\theta)\Gamma(\theta)} \int_0^s \mathfrak{w}^{\sigma-1} (s-\mathfrak{w})^{\theta-1} \alpha_1 \|L_1 - L_1^*\| \, d\mathfrak{w} \end{aligned}$$

$$\leq \left[\frac{(1-\theta)\sigma S^{\sigma-1}}{\mathcal{AB}(\theta)} + \frac{\theta\sigma S^{\theta+\sigma-1}\Gamma(\sigma)}{\mathcal{AB}(\theta)\Gamma(\theta+\sigma)} \right] \alpha_1 \|L_1 - L_1^*\|,$$

and so

$$\left(1 - \left[\frac{(1-\theta)\sigma S^{\sigma-1}}{\mathcal{AB}(\theta)} + \frac{\theta\sigma S^{\theta+\sigma-1}\Gamma(\sigma)}{\mathcal{AB}(\theta)\Gamma(\theta+\sigma)} \right] \alpha_1 \right) \|L_1 - L_1^*\| \leq 0.$$

From (23), we can assert that the above inequality holds if $\|L_1 - L_1^*\| = 0$ or $L_1 = L_1^*$. Similarly, from

$$\|L_2 - L_2^*\| \leq \left[\frac{(1-\theta)\sigma S^{\sigma-1}}{\mathcal{AB}(\theta)} + \frac{\theta\sigma S^{\theta+\sigma-1}\Gamma(\sigma)}{\mathcal{AB}(\theta)\Gamma(\theta+\sigma)} \right] \alpha_2 \|L_2 - L_2^*\|,$$

we obtain

$$\left(1 - \left[\frac{(1-\theta)\sigma S^{\sigma-1}}{\mathcal{AB}(\theta)} + \frac{\theta\sigma S^{\theta+\sigma-1}\Gamma(\sigma)}{\mathcal{AB}(\theta)\Gamma(\theta+\sigma)} \right] \alpha_2 \right) \|L_2 - L_2^*\| \leq 0,$$

which gives $\|L_2 - L_2^*\| = 0$ or $L_2 = L_2^*$. Furthermore,

$$\|L_3 - L_3^*\| \leq \left[\frac{(1-\theta)\sigma S^{\sigma-1}}{\mathcal{AB}(\theta)} + \frac{\theta\sigma S^{\theta+\sigma-1}\Gamma(\sigma)}{\mathcal{AB}(\theta)\Gamma(\theta+\sigma)} \right] \alpha_3 \|L_3 - L_3^*\|,$$

which yields

$$\left(1 - \left[\frac{(1-\theta)\sigma S^{\sigma-1}}{\mathcal{AB}(\theta)} + \frac{\theta\sigma S^{\theta+\sigma-1}\Gamma(\sigma)}{\mathcal{AB}(\theta)\Gamma(\theta+\sigma)} \right] \alpha_3 \right) \|L_3 - L_3^*\| \leq 0.$$

Hence, $L_3 = L_3^*$. As a consequence,

$$(L_1(s), L_2(s), L_3(s)) = (L_1^*(s), L_2^*(s), L_3^*(s)),$$

which proves that the solution to the fractal-fractional polluted lake system (4) is unique. \square

5 Ulam–Hyers–Rassias stability

In this section, the stability of the solutions to the polluted lake system of three lakes is studied. Given the desire to establish robust mathematical foundations for the model, we consider four different notions of stability. More precisely, we prove stability for our fractal-fractional (FF) polluted lake system (4) with respect to Ulam–Hyers and Ulam–Hyers–Rassias notions and their respective generalizations. Stability analysis is pivotal in ensuring mathematical models' reliability and predictability, especially in real-world applications such as the polluted lake system. Ulam stability, Hyers stability, and their generalizations offer valuable frameworks for understanding the behavior of solutions to dynamic systems under perturbations. Given the intricate nature of fractal-fractional systems, the use of these stability notions allows us to ascertain the system's resilience to variations and disturbances, providing insights into the long-term behavior and reliability of the proposed model. By choosing stability in this context, we aim to enhance the credibility of the model and its applicability in addressing the complexities inherent in polluted lake systems.

Definition 7. *The FF polluted lake system (4) is Ulam–Hyers stable if there exists $a_{\mathbb{Q}_1}$, $a_{\mathbb{Q}_2}$, $a_{\mathbb{Q}_3} \in \mathbb{R}^+$ such that for all $r_j > 0$, $j = 1, 2, 3$, and for all $(L_1^*, L_2^*, L_3^*) \in \mathbb{X}$ satisfying*

$$\begin{cases} \left| \mathbf{FFML} \mathcal{D}_{0,s}^{(\theta,\sigma)} L_1^*(s) - \mathbb{Q}_1(s, L_1^*(s), L_2^*(s), L_3^*(s)) \right| < r_1, \\ \left| \mathbf{FFML} \mathcal{D}_{0,s}^{(\theta,\sigma)} L_2^*(s) - \mathbb{Q}_2(s, L_1^*(s), L_2^*(s), L_3^*(s)) \right| < r_2, \\ \left| \mathbf{FFML} \mathcal{D}_{0,s}^{(\theta,\sigma)} L_3^*(s) - \mathbb{Q}_3(s, L_1^*(s), L_2^*(s), L_3^*(s)) \right| < r_3, \end{cases} \quad (24)$$

there exists $(L_1, L_2, L_3) \in \mathbb{X}$ satisfying the fractal-fractional polluted lake system (4) with

$$\begin{cases} |L_1^*(s) - L_1(s)| \leq a_{Q_1} r_1, \\ |L_2^*(s) - L_2(s)| \leq a_{Q_2} r_2, \\ |L_3^*(s) - L_3(s)| \leq a_{Q_3} r_3. \end{cases}$$

Definition 8. The FF polluted lake system (4) is generalized Ulam–Hyers stable if $\exists a_{Q_j} \in C(\mathbb{R}^+, \mathbb{R}^+)$, $j \in \{1, 2, 3\}$, with $a_{Q_j}(0) = 0$ such that $\forall r_j > 0$ and $\forall (L_1^*, L_2^*, L_3^*) \in \mathbb{X}$ fulfilling (24), there is a solution $(L_1, L_2, L_3) \in \mathbb{X}$ of the given FF polluted lake system (4) such that

$$\begin{cases} |L_1^*(s) - L_1(s)| \leq a_{Q_1}(r_1), \\ |L_2^*(s) - L_2(s)| \leq a_{Q_2}(r_2), \\ |L_3^*(s) - L_3(s)| \leq a_{Q_3}(r_3). \end{cases}$$

Remark 9. The triplet $(L_1^*, L_2^*, L_3^*) \in \mathbb{X}$ is a solution for (24) if, and only if, $\exists z_1, z_2, z_3 \in C([0, S], \mathbb{R})$ (each of them depend on L_1^*, L_2^*, L_3^* , respectively) such that $\forall s \in \mathbb{J}$,

(i) $|z_j(s)| < r_j$,

(ii) one has

$$\begin{cases} \mathbf{FFML}\mathcal{D}_{0,s}^{(\theta,\sigma)} L_1^*(s) = \mathbb{Q}_1(s, L_1^*(s), L_2^*(s), L_3^*(s)) + z_1(s), \\ \mathbf{FFML}\mathcal{D}_{0,s}^{(\theta,\sigma)} L_2^*(s) = \mathbb{Q}_2(s, L_1^*(s), L_2^*(s), L_3^*(s)) + z_2(s), \\ \mathbf{FFML}\mathcal{D}_{0,s}^{(\theta,\sigma)} L_3^*(s) = \mathbb{Q}_3(s, L_1^*(s), L_2^*(s), L_3^*(s)) + z_3(s). \end{cases}$$

Definition 10. The fractal-fractional polluted lake model (4) is Ulam–Hyers–Rassias stable with respect to \hbar_j , $j \in \{1, 2, 3\}$, if $\exists 0 < a_{(Q_j, \hbar_j)} \in \mathbb{R}$ such that $\forall r_j > 0$ and $\forall (L_1^*, L_2^*, L_3^*) \in \mathbb{X}$ fulfilling

$$\begin{cases} \left| \mathbf{FFML}\mathcal{D}_{0,s}^{(\theta,\sigma)} L_1^*(s) - \mathbb{Q}_1(s, L_1^*(s), L_2^*(s), L_3^*(s)) \right| < r_1 \hbar_1(s), \\ \left| \mathbf{FFML}\mathcal{D}_{0,s}^{(\theta,\sigma)} L_2^*(s) - \mathbb{Q}_2(s, L_1^*(s), L_2^*(s), L_3^*(s)) \right| < r_2 \hbar_2(s), \\ \left| \mathbf{FFML}\mathcal{D}_{0,s}^{(\theta,\sigma)} L_3^*(s) - \mathbb{Q}_3(s, L_1^*(s), L_2^*(s), L_3^*(s)) \right| < r_3 \hbar_3(s), \end{cases} \quad (25)$$

there exists a solution $(L_1, L_2, L_3) \in \mathbb{X}$ of the FF-model of polluted lake system (4) such that

$$\begin{cases} |L_1^*(s) - L_1(s)| \leq r_1 a_{(Q_1, \hbar_1)} \hbar_1(s), & \forall s \in \mathbb{J}, \\ |L_2^*(s) - L_2(s)| \leq r_2 a_{(Q_2, \hbar_2)} \hbar_2(s), & \forall s \in \mathbb{J}, \\ |L_3^*(s) - L_3(s)| \leq r_3 a_{(Q_3, \hbar_3)} \hbar_3(s), & \forall s \in \mathbb{J}, \end{cases}$$

with $\hbar_1, \hbar_2, \hbar_3 \in C([0, S], \mathbb{R}^+)$.

Remark 11. If $\hbar_j(s) = 1$, then Definition 10 reduces to the Ulam–Hyers criterion.

Definition 12. *The FF polluted lake system (4) is generalized Ulam–Hyers–Rasias stable with respect to \hbar_j if exists $a_{(\mathbb{Q}_j, \hbar_j)} \in C(\mathbb{R}^+, \mathbb{R}^+)$ such that for all $(L_1^*, L_2^*, L_3^*) \in \mathbb{X}$ satisfying*

$$\begin{cases} \left| \mathbf{FFML}\mathcal{D}_{0,s}^{(\theta,\sigma)} L_1^*(s) - \mathbb{Q}_1(s, L_1^*(s), L_2^*(s), L_3^*(s)) \right| < \hbar_1(s), \\ \left| \mathbf{FFML}\mathcal{D}_{0,s}^{(\theta,\sigma)} L_2^*(s) - \mathbb{Q}_2(s, L_1^*(s), L_2^*(s), L_3^*(s)) \right| < \hbar_2(s), \\ \left| \mathbf{FFML}\mathcal{D}_{0,s}^{(\theta,\sigma)} L_3^*(s) - \mathbb{Q}_3(s, L_1^*(s), L_2^*(s), L_3^*(s)) \right| < \hbar_3(s), \end{cases}$$

there exists a solution $(L_1, L_2, L_3) \in \mathbb{X}$ of the FF-model of polluted lake system (4) such that

$$\begin{cases} |L_1^*(s) - L_1(s)| \leq a_{(\mathbb{Q}_1, \hbar_1)}(r_1)\hbar_1(s), \\ |L_2^*(s) - L_2(s)| \leq a_{(\mathbb{Q}_2, \hbar_2)}(r_2)\hbar_2(s), \\ |L_3^*(s) - L_3(s)| \leq a_{(\mathbb{Q}_3, \hbar_3)}(r_3)\hbar_3(s). \end{cases}$$

Remark 13. *Note that $(L_1^*, L_2^*, L_3^*) \in \mathbb{X}$ is a solution for (25) if, and only if, $\exists z_1, z_2, z_3 \in C([0, S], \mathbb{R})$ (each of them depend on L_1^*, L_2^*, L_3^* , respectively) such that $\forall s \in \mathbb{J}$,*

(i) $|z_j(s)| < r_j \hbar_j(s)$,

(ii) we have

$$\begin{cases} \mathbf{FFML}\mathcal{D}_{0,s}^{(\theta,\sigma)} L_1^*(s) = \mathbb{Q}_1(s, L_1^*(s), L_2^*(s), L_3^*(s)) + z_1(s), \\ \mathbf{FFML}\mathcal{D}_{0,s}^{(\theta,\sigma)} L_2^*(s) = \mathbb{Q}_2(s, L_1^*(s), L_2^*(s), L_3^*(s)) + z_2(s), \\ \mathbf{FFML}\mathcal{D}_{0,s}^{(\theta,\sigma)} L_3^*(s) = \mathbb{Q}_3(s, L_1^*(s), L_2^*(s), L_3^*(s)) + z_3(s). \end{cases}$$

Lemmas 14 and 15 are useful to prove Theorems 16 and 17, respectively.

Lemma 14. *For each $r_1, r_2, r_3 > 0$, suppose that $(L_1^*, L_2^*, L_3^*) \in \mathbb{X}$ is a solution of (24). Then, functions $L_1^*, L_2^*, L_3^* \in \mathbb{C}$ fulfill the following three inequalities:*

$$\begin{aligned} & \left| L_1^*(s) - \left(L_{1,0} + \frac{(1-\theta)\sigma s^{\sigma-1}}{\mathcal{AB}(\theta)} \mathbb{Q}_1(s, L_1^*(s), L_2^*(s), L_3^*(s)) + \frac{\theta\sigma}{\mathcal{AB}(\theta)\Gamma(\theta)} \int_0^s \mathfrak{w}^{\sigma-1} (s-\mathfrak{w})^{\theta-1} \right. \right. \\ & \quad \left. \left. \times \mathbb{Q}_1(\mathfrak{w}, L_1^*(\mathfrak{w}), L_2^*(\mathfrak{w}), L_3^*(\mathfrak{w})) d\mathfrak{w} \right) \right| \leq \left[\frac{(1-\theta)\sigma S^{\sigma-1}}{\mathcal{AB}(\theta)} + \frac{\theta\sigma S^{\theta+\sigma-1}\Gamma(\sigma)}{\mathcal{AB}(\theta)\Gamma(\theta+\sigma)} \right] r_1, \end{aligned} \quad (26)$$

$$\begin{aligned} & \left| L_2^*(s) - \left(L_{2,0} + \frac{(1-\theta)\sigma s^{\sigma-1}}{\mathcal{AB}(\theta)} \mathbb{Q}_2(s, L_1^*(s), L_2^*(s), L_3^*(s)) + \frac{\theta\sigma}{\mathcal{AB}(\theta)\Gamma(\theta)} \int_0^s \mathfrak{w}^{\sigma-1} (s-\mathfrak{w})^{\theta-1} \right. \right. \\ & \quad \left. \left. \times \mathbb{Q}_2(\mathfrak{w}, L_1^*(\mathfrak{w}), L_2^*(\mathfrak{w}), L_3^*(\mathfrak{w})) d\mathfrak{w} \right) \right| \leq \left[\frac{(1-\theta)\sigma S^{\sigma-1}}{\mathcal{AB}(\theta)} + \frac{\theta\sigma S^{\theta+\sigma-1}\Gamma(\sigma)}{\mathcal{AB}(\theta)\Gamma(\theta+\sigma)} \right] r_2, \end{aligned} \quad (27)$$

and

$$\begin{aligned} & \left| L_3^*(s) - \left(L_{3,0} + \frac{(1-\theta)\sigma s^{\sigma-1}}{\mathcal{AB}(\theta)} \mathbb{Q}_3(s, L_1^*(s), L_2^*(s), L_3^*(s)) + \frac{\theta\sigma}{\mathcal{AB}(\theta)\Gamma(\theta)} \int_0^s \mathfrak{w}^{\sigma-1} (s-\mathfrak{w})^{\theta-1} \right. \right. \\ & \quad \left. \left. \times \mathbb{Q}_3(\mathfrak{w}, L_1^*(\mathfrak{w}), L_2^*(\mathfrak{w}), L_3^*(\mathfrak{w})) d\mathfrak{w} \right) \right| \leq \left[\frac{(1-\theta)\sigma S^{\sigma-1}}{\mathcal{AB}(\theta)} + \frac{\theta\sigma S^{\theta+\sigma-1}\Gamma(\sigma)}{\mathcal{AB}(\theta)\Gamma(\theta+\sigma)} \right] r_3. \end{aligned} \quad (28)$$

Proof. Let $r_1 > 0$ be arbitrary. Since $L_1^* \in \mathbb{C}$ satisfies

$$\left| \mathbf{FFML} \mathcal{D}_{0,s}^{(\theta,\sigma)} L_1^*(s) - \mathbb{Q}_1(s, L_1^*(s), L_2^*(s), L_3^*(s)) \right| < r_1,$$

it follows from Remark 9 that one can take a function $z_1(s)$ such that

$$\mathbf{FFML} \mathcal{D}_{0,s}^{(\theta,\sigma)} L_1^*(s) = \mathbb{Q}_1(s, L_1^*(s), L_2^*(s), L_3^*(s)) + z_1(s)$$

and $|z_1(s)| \leq r_1$. Clearly,

$$\begin{aligned} L_1^*(s) &= L_{1,0} + \frac{(1-\theta)\sigma s^{\sigma-1}}{\mathcal{AB}(\theta)} [\mathbb{Q}_1(s, L_1^*(s), L_2^*(s), L_3^*(s)) + z_1(s)] \\ &\quad + \frac{\theta\sigma}{\mathcal{AB}(\theta)\Gamma(\theta)} \int_0^s \mathfrak{w}^{\sigma-1} (s-\mathfrak{w})^{\theta-1} [\mathbb{Q}_1(\mathfrak{w}, L_1^*(\mathfrak{w}), L_2^*(\mathfrak{w}), L_3^*(\mathfrak{w})) + z_1(\mathfrak{w})] d\mathfrak{w}. \end{aligned}$$

In this case, we estimate

$$\begin{aligned} &\left| L_1^*(s) - \left(L_{1,0} + \frac{(1-\theta)\sigma s^{\sigma-1}}{\mathcal{AB}(\theta)} \mathbb{Q}_1(s, L_1^*(s), L_2^*(s), L_3^*(s)) \right. \right. \\ &\quad \left. \left. + \frac{\theta\sigma}{\mathcal{AB}(\theta)\Gamma(\theta)} \int_0^s \mathfrak{w}^{\sigma-1} (s-\mathfrak{w})^{\theta-1} \mathbb{Q}_1(\mathfrak{w}, L_1^*(\mathfrak{w}), L_2^*(\mathfrak{w}), L_3^*(\mathfrak{w})) d\mathfrak{w} \right) \right| \\ &\leq \frac{(1-\theta)\sigma s^{\sigma-1}}{\mathcal{AB}(\theta)} |z_1(s)| + \frac{\theta\sigma}{\mathcal{AB}(\theta)\Gamma(\theta)} \int_0^s \mathfrak{w}^{\sigma-1} (s-\mathfrak{w})^{\theta-1} |z_1(\mathfrak{w})| d\mathfrak{w} \\ &\leq \frac{(1-\theta)\sigma S^{\sigma-1}}{\mathcal{AB}(\theta)} r_1 + \frac{\theta\sigma S^{\theta+\sigma-1}\Gamma(\sigma)}{\mathcal{AB}(\theta)\Gamma(\theta+\sigma)} r_1 \\ &= \left[\frac{(1-\theta)\sigma S^{\sigma-1}}{\mathcal{AB}(\theta)} + \frac{\theta\sigma S^{\theta+\sigma-1}\Gamma(\sigma)}{\mathcal{AB}(\theta)\Gamma(\theta+\sigma)} \right] r_1. \end{aligned}$$

This means that (26) is fulfilled. We prove (27) and (28) in a similar way. \square

To prove our next result (see Lemma 15), we consider the following condition:

(C2) there exists increasing mappings $\hbar_j \in C([0, S], \mathbb{R}^+)$, $j \in \{1, 2, 3\}$, and $\Delta_{\hbar_j} > 0$, provided that

$$\mathbf{FFML} \mathcal{I}_{0,s}^{(\theta,\sigma)} \hbar_j(s) < \Delta_{\hbar_j} \hbar_j(s), \quad (j \in \{1, 2, 3\}), \forall s \in \mathbb{J}. \quad (29)$$

Lemma 15. *Let (C2) hold. For each $r_1, r_2, r_3 > 0$, suppose that $(L_1^*, L_2^*, L_3^*) \in \mathbb{X}$ is a solution of (25). Then, functions $L_1^*, L_2^*, L_3^* \in \mathbb{C}$ fulfill the following three inequalities:*

$$\left| L_1^*(s) - \left(L_{1,0} + \mathbf{FFML} \mathcal{I}_{0,s}^{(\theta,\sigma)} \mathbb{Q}_1(s, L_1^*(s), L_2^*(s), L_3^*(s)) \right) \right| \leq r_1 \Delta_{\hbar_1} \hbar_1(s), \quad (30)$$

$$\left| L_2^*(s) - \left(L_{2,0} + \mathbf{FFML} \mathcal{I}_{0,s}^{(\theta,\sigma)} \mathbb{Q}_2(s, L_1^*(s), L_2^*(s), L_3^*(s)) \right) \right| \leq r_2 \Delta_{\hbar_2} \hbar_2(s), \quad (31)$$

$$\left| L_3^*(s) - \left(L_{3,0} + \mathbf{FFML} \mathcal{I}_{0,s}^{(\theta,\sigma)} \mathbb{Q}_3(s, L_1^*(s), L_2^*(s), L_3^*(s)) \right) \right| \leq r_3 \Delta_{\hbar_3} \hbar_3(s). \quad (32)$$

Proof. Let $r_1 > 0$. Since $L_1^* \in \mathbb{C}$ satisfies

$$\left| \mathbf{FFML} \mathcal{D}_{0,s}^{(\theta,\sigma)} L_1^*(s) - \mathbb{Q}_1(s, L_1^*(s), L_2^*(s), L_3^*(s)) \right| < r_1 \hbar_1(s),$$

it follows from Remark 13 that we can take $z_1(s)$ such that

$$\mathbf{FFML}\mathcal{D}_{0,s}^{(\theta,\sigma)}L_1^*(s) = \mathbb{Q}_1(s, L_1^*(s), L_2^*(s), L_3^*(s)) + z_1(s)$$

and $|z_1(s)| \leq r_1 \hat{h}_1(s)$. Evidently,

$$\begin{aligned} L_1^*(s) &= L_{1,0} + \frac{(1-\theta)\sigma s^{\sigma-1}}{\mathcal{AB}(\theta)} [\mathbb{Q}_1(s, L_1^*(s), L_2^*(s), L_3^*(s)) + z_1(s)] \\ &\quad + \frac{\theta\sigma}{\mathcal{AB}(\theta)\Gamma(\theta)} \int_0^s \mathfrak{w}^{\sigma-1} (s-\mathfrak{w})^{\theta-1} [\mathbb{Q}_1(\mathfrak{w}, L_1^*(\mathfrak{w}), L_2^*(\mathfrak{w}), L_3^*(\mathfrak{w})) + z_1(\mathfrak{w})] d\mathfrak{w}. \end{aligned}$$

Then, we estimate

$$\begin{aligned} &\left| L_1^*(s) - \left(L_{1,0} + \mathbf{FFML}\mathcal{T}_{0,s}^{(\theta,\sigma)}\mathbb{Q}_1(s, L_1^*(s), L_2^*(s), L_3^*(s)) \right) \right| \\ &= \left| L_1^*(s) - \left(L_{1,0} + \frac{(1-\theta)\sigma s^{\sigma-1}}{\mathcal{AB}(\theta)} \mathbb{Q}_1(s, L_1^*(s), L_2^*(s), L_3^*(s)) \right. \right. \\ &\quad \left. \left. + \frac{\theta\sigma}{\mathcal{AB}(\theta)\Gamma(\theta)} \int_0^s \mathfrak{w}^{\sigma-1} (s-\mathfrak{w})^{\theta-1} \mathbb{Q}_1(\mathfrak{w}, L_1^*(\mathfrak{w}), L_2^*(\mathfrak{w}), L_3^*(\mathfrak{w})) d\mathfrak{w} \right) \right| \\ &\leq \frac{(1-\theta)\sigma s^{\sigma-1}}{\mathcal{AB}(\theta)} |z_1(s)| + \frac{\theta\sigma}{\mathcal{AB}(\theta)\Gamma(\theta)} \int_0^s \mathfrak{w}^{\sigma-1} (s-\mathfrak{w})^{\theta-1} |z_1(\mathfrak{w})| d\mathfrak{w} \\ &= \mathbf{FFML}\mathcal{T}_{0,s}^{(\theta,\sigma)} |z_1(s)| \\ &\leq \mathbf{FFML}\mathcal{T}_{0,s}^{(\theta,\sigma)} r_1 \hat{h}_1(s) \\ &\leq r_1 \Delta_{\hat{h}_1} \hat{h}_1(s). \end{aligned}$$

We prove the remaining inequalities in a similar way. \square

We are now in a position to investigate the Ulam–Hyers stability for the FF-model of polluted lake system (4).

Theorem 16. *Assume (C1) holds. Then our polluted lake system (4) is both Ulam–Hyers and generalized Ulam–Hyers stable with*

$$\left[\frac{(1-\theta)\sigma S^{\sigma-1}}{\mathcal{AB}(\theta)} + \frac{\theta\sigma S^{\theta+\sigma-1}\Gamma(\sigma)}{\mathcal{AB}(\theta)\Gamma(\theta+\sigma)} \right] \alpha_j < 1, \quad j \in \{1, 2, 3\},$$

in which $\alpha_1, \alpha_2, \alpha_3 > 0$ are given by (21).

Proof. Let $r_1 > 0$ and $L_1^* \in \mathbb{C}$ be an arbitrary solution of (24). By Theorem 6, let $L_1 \in \mathbb{C}$ be the unique solution of the FF polluted lake system (4). Then $L_1(s)$ is defined as

$$\begin{aligned} L_1(s) &= L_{1,0} + \frac{(1-\theta)\sigma s^{\sigma-1}}{\mathcal{AB}(\theta)} \mathbb{Q}_1(s, L_1(s), L_2(s), L_3(s)) \\ &\quad + \frac{\theta\sigma}{\mathcal{AB}(\theta)\Gamma(\theta)} \int_0^s \mathfrak{w}^{\sigma-1} (s-\mathfrak{w})^{\theta-1} \mathbb{Q}_1(\mathfrak{w}, L_1(\mathfrak{w}), L_2(\mathfrak{w}), L_3(\mathfrak{w})) d\mathfrak{w}. \end{aligned}$$

From the triangle inequality, Lemma 14 gives

$$|L_1^*(s) - L_1(s)| \leq \left| L_1^*(s) - L_{1,0} - \frac{(1-\theta)\sigma s^{\sigma-1}}{\mathcal{AB}(\theta)} \mathbb{Q}_1(s, L_1(s), L_2(s), L_3(s)) \right|$$

$$\begin{aligned}
 & - \frac{\theta\sigma}{\mathcal{AB}(\theta)\Gamma(\theta)} \int_0^s \mathfrak{w}^{\sigma-1} (s-\mathfrak{w})^{\theta-1} \mathbb{Q}_1(\mathfrak{w}, L_1(\mathfrak{w}), L_2(\mathfrak{w}), L_3(\mathfrak{w})) \, d\mathfrak{w} \Big| \\
 & \leq \left| L_1^*(s) - \left(L_{1,0} + \frac{(1-\theta)\sigma s^{\sigma-1}}{\mathcal{AB}(\theta)} \mathbb{Q}_1(s, L_1^*(s), L_2^*(s), L_3^*(s)) \right. \right. \\
 & \quad \left. \left. + \frac{\theta\sigma}{\mathcal{AB}(\theta)\Gamma(\theta)} \int_0^s \mathfrak{w}^{\sigma-1} (s-\mathfrak{w})^{\theta-1} \mathbb{Q}_1(\mathfrak{w}, L_1^*(\mathfrak{w}), L_2^*(\mathfrak{w}), L_3^*(\mathfrak{w})) \, d\mathfrak{w} \right) \right| \\
 & \quad + \frac{(1-\theta)\sigma s^{\sigma-1}}{\mathcal{AB}(\theta)} \left| \mathbb{Q}_1(s, L_1^*(s), L_2^*(s), L_3^*(s)) - \mathbb{Q}_1(s, L_1(s), L_2(s), L_3(s)) \right| \\
 & \quad + \frac{\theta\sigma}{\mathcal{AB}(\theta)\Gamma(\theta)} \int_0^s \mathfrak{w}^{\sigma-1} (s-\mathfrak{w})^{\theta-1} \left| \mathbb{Q}_1(\mathfrak{w}, L_1^*(\mathfrak{w}), L_2^*(\mathfrak{w}), L_3^*(\mathfrak{w})) \right. \\
 & \quad \left. - \mathbb{Q}_1(\mathfrak{w}, L_1(\mathfrak{w}), L_2(\mathfrak{w}), L_3(\mathfrak{w})) \right| \, d\mathfrak{w} \\
 & \leq \left[\frac{(1-\theta)\sigma S^{\sigma-1}}{\mathcal{AB}(\theta)} + \frac{\theta\sigma S^{\theta+\sigma-1}\Gamma(\sigma)}{\mathcal{AB}(\theta)\Gamma(\theta+\sigma)} \right] r_1 + \frac{(1-\theta)\sigma S^{\sigma-1}}{\mathcal{AB}(\theta)} \alpha_1 \|L_1^* - L_1\| \\
 & \quad + \frac{\theta\sigma S^{\theta+\sigma-1}\Gamma(\sigma)}{\mathcal{AB}(\theta)\Gamma(\theta+\sigma)} \alpha_1 \|L_1^* - L_1\| \\
 & \leq \left[\frac{(1-\theta)\sigma S^{\sigma-1}}{\mathcal{AB}(\theta)} + \frac{\theta\sigma S^{\theta+\sigma-1}\Gamma(\sigma)}{\mathcal{AB}(\theta)\Gamma(\theta+\sigma)} \right] r_1 + \left[\frac{(1-\theta)\sigma S^{\sigma-1}}{\mathcal{AB}(\theta)} + \frac{\theta\sigma S^{\theta+\sigma-1}\Gamma(\sigma)}{\mathcal{AB}(\theta)\Gamma(\theta+\sigma)} \right] \alpha_1 \|L_1 - L_1^*\|.
 \end{aligned}$$

Hence,

$$\|L_1^* - L_1\| \leq \frac{\left[\frac{(1-\theta)\sigma S^{\sigma-1}}{\mathcal{AB}(\theta)} + \frac{\theta\sigma S^{\theta+\sigma-1}\Gamma(\sigma)}{\mathcal{AB}(\theta)\Gamma(\theta+\sigma)} \right] r_1}{1 - \left[\frac{(1-\theta)\sigma S^{\sigma-1}}{\mathcal{AB}(\theta)} + \frac{\theta\sigma S^{\theta+\sigma-1}\Gamma(\sigma)}{\mathcal{AB}(\theta)\Gamma(\theta+\sigma)} \right] \alpha_1}.$$

Set $a_{\mathbb{Q}_1} = \frac{\left[\frac{(1-\theta)\sigma S^{\sigma-1}}{\mathcal{AB}(\theta)} + \frac{\theta\sigma S^{\theta+\sigma-1}\Gamma(\sigma)}{\mathcal{AB}(\theta)\Gamma(\theta+\sigma)} \right]}{1 - \left[\frac{(1-\theta)\sigma S^{\sigma-1}}{\mathcal{AB}(\theta)} + \frac{\theta\sigma S^{\theta+\sigma-1}\Gamma(\sigma)}{\mathcal{AB}(\theta)\Gamma(\theta+\sigma)} \right] \alpha_1}$. In this case, $\|L_1^* - L_1\| \leq a_{\mathbb{Q}_1} r_1$. Similarly,

we obtain

$$\begin{aligned}
 \|L_2^* - L_2\| & \leq a_{\mathbb{Q}_2} r_2, \\
 \|L_3^* - L_3\| & \leq a_{\mathbb{Q}_3} r_3,
 \end{aligned}$$

where

$$a_{\mathbb{Q}_j} = \frac{\left[\frac{(1-\theta)\sigma S^{\sigma-1}}{\mathcal{AB}(\theta)} + \frac{\theta\sigma S^{\theta+\sigma-1}\Gamma(\sigma)}{\mathcal{AB}(\theta)\Gamma(\theta+\sigma)} \right]}{1 - \left[\frac{(1-\theta)\sigma S^{\sigma-1}}{\mathcal{AB}(\theta)} + \frac{\theta\sigma S^{\theta+\sigma-1}\Gamma(\sigma)}{\mathcal{AB}(\theta)\Gamma(\theta+\sigma)} \right] \alpha_j}, \quad j \in \{2, 3\}.$$

We conclude that the FF-model of polluted lake system (4) is Ulam–Hyers stable. On the other hand, if we take

$$a_{\mathbb{Q}_j}(r_j) = \frac{\left[\frac{(1-\theta)\sigma S^{\sigma-1}}{\mathcal{AB}(\theta)} + \frac{\theta\sigma S^{\theta+\sigma-1}\Gamma(\sigma)}{\mathcal{AB}(\theta)\Gamma(\theta+\sigma)} \right] r_j}{1 - \left[\frac{(1-\theta)\sigma S^{\sigma-1}}{\mathcal{AB}(\theta)} + \frac{\theta\sigma S^{\theta+\sigma-1}\Gamma(\sigma)}{\mathcal{AB}(\theta)\Gamma(\theta+\sigma)} \right] \alpha_j}, \quad j \in \{1, 2, 3\},$$

then $a_{\mathbb{Q}_j}(0) = 0$ and the proof is finished: (4) is generalized Ulam–Hyers stable. \square

Theorem 17 establishes Ulam–Hyers–Rassias stability for the fractal-fractional polluted lake system (4).

Theorem 17. *If (C1) and (C2) hold, then the FF-model of polluted lake system (4) is simultaneously stable in the sense of Definitions 7 and 8.*

Proof. Let $r_1 > 0$, and $L_1^* \in \mathbb{C}$ satisfy (25). By Theorem 6, let $L_1 \in \mathbb{C}$ be the (unique) solution of the FF polluted lake system model (4). Then $L_1(s)$ becomes

$$\begin{aligned} L_1(s) &= L_{1,0} + \frac{(1-\theta)\sigma s^{\sigma-1}}{\mathcal{AB}(\theta)} \mathbb{Q}_1(s, L_1(s), L_2(s), L_3(s)) \\ &\quad + \frac{\theta\sigma}{\mathcal{AB}(\theta)\Gamma(\theta)} \int_0^s \mathfrak{w}^{\sigma-1} (s-\mathfrak{w})^{\theta-1} \mathbb{Q}_1(\mathfrak{w}, L_1(\mathfrak{w}), L_2(\mathfrak{w}), L_3(\mathfrak{w})) \, d\mathfrak{w}. \end{aligned}$$

With the aid of the triangle inequality, Lemma 15 gives

$$\begin{aligned} |L_1^*(s) - L_1(s)| &\leq \left| L_1^*(s) - L_{1,0} - \frac{(1-\theta)\sigma s^{\sigma-1}}{\mathcal{AB}(\theta)} \mathbb{Q}_1(s, L_1(s), L_2(s), L_3(s)) \right. \\ &\quad \left. - \frac{\theta\sigma}{\mathcal{AB}(\theta)\Gamma(\theta)} \int_0^s \mathfrak{w}^{\sigma-1} (s-\mathfrak{w})^{\theta-1} \mathbb{Q}_1(\mathfrak{w}, L_1(\mathfrak{w}), L_2(\mathfrak{w}), L_3(\mathfrak{w})) \, d\mathfrak{w} \right| \\ &\leq \left| L_1^*(s) - \left(L_{1,0} + \frac{(1-\theta)\sigma s^{\sigma-1}}{\mathcal{AB}(\theta)} \mathbb{Q}_1(s, L_1^*(s), L_2^*(s), L_3^*(s)) \right. \right. \\ &\quad \left. \left. + \frac{\theta\sigma}{\mathcal{AB}(\theta)\Gamma(\theta)} \int_0^s \mathfrak{w}^{\sigma-1} (s-\mathfrak{w})^{\theta-1} \mathbb{Q}_1(\mathfrak{w}, L_1^*(\mathfrak{w}), L_2^*(\mathfrak{w}), L_3^*(\mathfrak{w})) \, d\mathfrak{w} \right) \right| \\ &\quad + \frac{(1-\theta)\sigma s^{\sigma-1}}{\mathcal{AB}(\theta)} \left| \mathbb{Q}_1(s, L_1^*(s), L_2^*(s), L_3^*(s)) - \mathbb{Q}_1(s, L_1(s), L_2(s), L_3(s)) \right| \\ &\quad + \frac{\theta\sigma}{\mathcal{AB}(\theta)\Gamma(\theta)} \int_0^s \mathfrak{w}^{\sigma-1} (s-\mathfrak{w})^{\theta-1} \left| \mathbb{Q}_1(\mathfrak{w}, L_1^*(\mathfrak{w}), L_2^*(\mathfrak{w}), L_3^*(\mathfrak{w})) \right. \\ &\quad \left. - \mathbb{Q}_1(\mathfrak{w}, L_1(\mathfrak{w}), L_2(\mathfrak{w}), L_3(\mathfrak{w})) \right| \, d\mathfrak{w} \\ &\leq \left| L_1^*(s) - \left(L_{1,0} + \mathbf{FFML} \mathcal{I}_{0,s}^{(\theta,\sigma)} \mathbb{Q}_1(s, L_1^*(s), L_2^*(s), L_3^*(s)) \right) \right| \\ &\quad + \frac{(1-\theta)\sigma s^{\sigma-1}}{\mathcal{AB}(\theta)} \left| \mathbb{Q}_1(s, L_1^*(s), L_2^*(s), L_3^*(s)) - \mathbb{Q}_1(s, L_1(s), L_2(s), L_3(s)) \right| \\ &\quad + \frac{\theta\sigma}{\mathcal{AB}(\theta)\Gamma(\theta)} \int_0^s \mathfrak{w}^{\sigma-1} (s-\mathfrak{w})^{\theta-1} \left| \mathbb{Q}_1(\mathfrak{w}, L_1^*(\mathfrak{w}), L_2^*(\mathfrak{w}), L_3^*(\mathfrak{w})) \right. \\ &\quad \left. - \mathbb{Q}_1(\mathfrak{w}, L_1(\mathfrak{w}), L_2(\mathfrak{w}), L_3(\mathfrak{w})) \right| \, d\mathfrak{w} \\ &\leq r_1 \Delta_{\hbar_1} \hbar_1(s) + \frac{(1-\theta)\sigma S^{\sigma-1}}{\mathcal{AB}(\theta)} \alpha_1 \|L_1^* - L_1\| + \frac{\theta\sigma S^{\theta+\sigma-1} \Gamma(\sigma)}{\mathcal{AB}(\theta)\Gamma(\theta+\sigma)} \alpha_1 \|L_1^* - L_1\| \\ &\leq r_1 \Delta_{\hbar_1} \hbar_1(s) + \left[\frac{(1-\theta)\sigma S^{\sigma-1}}{\mathcal{AB}(\theta)} + \frac{\theta\sigma S^{\theta+\sigma-1} \Gamma(\sigma)}{\mathcal{AB}(\theta)\Gamma(\theta+\sigma)} \right] \alpha_1 \|L_1 - L_1^*\|. \end{aligned}$$

Accordingly, we obtain that

$$\|L_1^* - L_1\| \leq \frac{r_1 \Delta_{\tilde{h}_1} \tilde{h}_1(s)}{1 - \left[\frac{(1-\theta)\sigma S^{\sigma-1}}{\mathcal{AB}(\theta)} + \frac{\theta\sigma S^{\theta+\sigma-1}\Gamma(\sigma)}{\mathcal{AB}(\theta)\Gamma(\theta+\sigma)} \right] \alpha_1}.$$

Set

$$a_{(\mathbb{Q}_1, \tilde{h}_1)} = \frac{\Delta_{\tilde{h}_1}}{1 - \left[\frac{(1-\theta)\sigma S^{\sigma-1}}{\mathcal{AB}(\theta)} + \frac{\theta\sigma S^{\theta+\sigma-1}\Gamma(\sigma)}{\mathcal{AB}(\theta)\Gamma(\theta+\sigma)} \right] \alpha_1}.$$

Then $\|L_1^* - L_1\| \leq r_1 a_{(\mathbb{Q}_1, \tilde{h}_1)} \tilde{h}_1(s)$. Similarly,

$$\|L_2^* - L_2\| \leq r_2 a_{(\mathbb{Q}_2, \tilde{h}_2)} \tilde{h}_2(s),$$

$$\|L_3^* - L_3\| \leq r_3 a_{(\mathbb{Q}_3, \tilde{h}_3)} \tilde{h}_3(s),$$

where

$$a_{(\mathbb{Q}_j, \tilde{h}_j)} = \frac{\Delta_{\tilde{h}_j}}{1 - \left[\frac{(1-\theta)\sigma S^{\sigma-1}}{\mathcal{AB}(\theta)} + \frac{\theta\sigma S^{\theta+\sigma-1}\Gamma(\sigma)}{\mathcal{AB}(\theta)\Gamma(\theta+\sigma)} \right] \alpha_j}, \quad j \in \{2, 3\}.$$

As a consequence, the fractal-fractional polluted lake system (4) is stable in the sense of Definition 7. By defining $r_j = 1$, $j \in \{1, 2, 3\}$, our FF polluted lake system model (4) is also stable in the sense of Definition 8. \square

6 Numerical algorithm via the Adams–Bashforth method

The Adams–Bashforth method is a robust numerical integration technique commonly used for solving most differential equations. Its higher-order accuracy and efficiency make it particularly suitable for approximating the solution of dynamic systems, such as those describing the behavior of polluted lake systems. By choosing the Adams–Bashforth technique, we aim to achieve accurate and stable numerical solutions for the fractal-fractional polluted lake system (4).

To do this, we apply the fractional Adams–Bashforth technique with two-step Lagrange polynomials. For that we redefine the fractal-fractional integral equations (15) at s_{k+1} . Precisely, we discretize the integral equations (15) for $s = s_{k+1}$ as follows:

$$\left\{ \begin{array}{l} L_1(s_{k+1}) = L_{1,0} + \frac{(1-\theta)\sigma s_k^{\sigma-1}}{\mathcal{AB}(\theta)} \mathbb{Q}_1(s_k, L_1(s_k), L_2(s_k), L_3(s_k)) \\ \quad + \frac{\theta\sigma}{\mathcal{AB}(\theta)\Gamma(\theta)} \int_0^{s_{k+1}} \mathfrak{w}^{\sigma-1} (s_{k+1} - \mathfrak{w})^{\theta-1} \mathbb{Q}_1(\mathfrak{w}, L_1(\mathfrak{w}), L_2(\mathfrak{w}), L_3(\mathfrak{w})) \, d\mathfrak{w}, \\ L_2(s_{k+1}) = L_{2,0} + \frac{(1-\theta)\sigma s_k^{\sigma-1}}{\mathcal{AB}(\theta)} \mathbb{Q}_2(s_k, L_1(s_k), L_2(s_k), L_3(s_k)) \\ \quad + \frac{\theta\sigma}{\mathcal{AB}(\theta)\Gamma(\theta)} \int_0^{s_{k+1}} \mathfrak{w}^{\sigma-1} (s_{k+1} - \mathfrak{w})^{\theta-1} \mathbb{Q}_2(\mathfrak{w}, L_1(\mathfrak{w}), L_2(\mathfrak{w}), L_3(\mathfrak{w})) \, d\mathfrak{w}, \\ L_3(s_{k+1}) = L_{3,0} + \frac{(1-\theta)\sigma s_k^{\sigma-1}}{\mathcal{AB}(\theta)} \mathbb{Q}_3(s_k, L_1(s_k), L_2(s_k), L_3(s_k)) \\ \quad + \frac{\theta\sigma}{\mathcal{AB}(\theta)\Gamma(\theta)} \int_0^{s_{k+1}} \mathfrak{w}^{\sigma-1} (s_{k+1} - \mathfrak{w})^{\theta-1} \mathbb{Q}_3(\mathfrak{w}, L_1(\mathfrak{w}), L_2(\mathfrak{w}), L_3(\mathfrak{w})) \, d\mathfrak{w}. \end{array} \right.$$

The approximation of the above integrals are given by

$$\left\{ \begin{array}{l} L_1(s_{k+1}) = L_{1,0} + \frac{(1-\theta)\sigma s_k^{\sigma-1}}{\mathcal{AB}(\theta)} \mathbb{Q}_1(s_k, L_1(s_k), L_2(s_k), L_3(s_k)) \\ \quad + \frac{\theta\sigma}{\mathcal{AB}(\theta)\Gamma(\theta)} \sum_{\ell=1}^k \int_{s_\ell}^{s_{\ell+1}} \mathbf{w}^{\sigma-1} (s_{k+1} - \mathbf{w})^{\theta-1} \mathbb{Q}_1(\mathbf{w}, L_1(\mathbf{w}), L_2(\mathbf{w}), L_3(\mathbf{w})) \, d\mathbf{w}, \\ L_2(s_{k+1}) = L_{2,0} + \frac{(1-\theta)\sigma s_k^{\sigma-1}}{\mathcal{AB}(\theta)} \mathbb{Q}_2(s_k, L_1(s_k), L_2(s_k), L_3(s_k)) \\ \quad + \frac{\theta\sigma}{\mathcal{AB}(\theta)\Gamma(\theta)} \sum_{\ell=1}^k \int_{s_\ell}^{s_{\ell+1}} \mathbf{w}^{\sigma-1} (s_{k+1} - \mathbf{w})^{\theta-1} \mathbb{Q}_2(\mathbf{w}, L_1(\mathbf{w}), L_2(\mathbf{w}), L_3(\mathbf{w})) \, d\mathbf{w}, \\ L_3(s_{k+1}) = L_{3,0} + \frac{(1-\theta)\sigma s_k^{\sigma-1}}{\mathcal{AB}(\theta)} \mathbb{Q}_3(s_k, L_1(s_k), L_2(s_k), L_3(s_k)) \\ \quad + \frac{\theta\sigma}{\mathcal{AB}(\theta)\Gamma(\theta)} \sum_{\ell=1}^k \int_{s_\ell}^{s_{\ell+1}} \mathbf{w}^{\sigma-1} (s_{k+1} - \mathbf{w})^{\theta-1} \mathbb{Q}_3(\mathbf{w}, L_1(\mathbf{w}), L_2(\mathbf{w}), L_3(\mathbf{w})) \, d\mathbf{w}. \end{array} \right.$$

Next, we approximate $\mathbf{w}^{\sigma-1} \mathbb{Q}_j(\mathbf{w}, L_1(\mathbf{w}), L_2(\mathbf{w}), L_3(\mathbf{w}))$, $j = 1, 2, 3$, on $[s_\ell, s_{\ell+1}]$ by applying two-step Lagrange interpolation polynomials under the step size $\mathbf{h} = s_\ell - s_{\ell-1}$. By direct computations, we obtain the following algorithm that yields numerical solutions to the FF-model of polluted lake system (4):

$$\begin{aligned} L_{1,k+1} &= L_{1,0} + \frac{(1-\theta)\sigma s_k^{\sigma-1}}{\mathcal{AB}(\theta)} \mathbb{Q}_1(s_k, L_1, k, L_2, k, L_3, k) + \frac{\sigma \mathbf{h}^\theta}{\mathcal{AB}(\theta)\Gamma(\theta+2)} \\ &\quad \times \sum_{\ell=1}^k \left[s_\ell^{\sigma-1} \mathbb{Q}_1(s_\ell, L_{1,\ell}, L_{2,\ell}, L_{3,\ell}) \hat{Y}_1(k, \ell) - s_{\ell-1}^{\sigma-1} \mathbb{Q}_1(s_{\ell-1}, L_{1,\ell-1}, L_{2,\ell-1}, L_{3,\ell-1}) \hat{Y}_2(k, \ell) \right], \end{aligned} \quad (33)$$

$$\begin{aligned} L_{2,k+1} &= L_{2,0} + \frac{(1-\theta)\sigma s_k^{\sigma-1}}{\mathcal{AB}(\theta)} \mathbb{Q}_2(s_k, L_1, k, L_2, k, L_3, k) + \frac{\sigma \mathbf{h}^\theta}{\mathcal{AB}(\theta)\Gamma(\theta+2)} \\ &\quad \times \sum_{\ell=1}^k \left[s_\ell^{\sigma-1} \mathbb{Q}_2(s_\ell, L_{1,\ell}, L_{2,\ell}, L_{3,\ell}) \hat{Y}_1(k, \ell) - s_{\ell-1}^{\sigma-1} \mathbb{Q}_2(s_{\ell-1}, L_{1,\ell-1}, L_{2,\ell-1}, L_{3,\ell-1}) \hat{Y}_2(k, \ell) \right], \end{aligned} \quad (34)$$

$$\begin{aligned} L_{3,k+1} &= L_{3,0} + \frac{(1-\theta)\sigma s_k^{\sigma-1}}{\mathcal{AB}(\theta)} \mathbb{Q}_3(s_k, L_1, k, L_2, k, L_3, k) + \frac{\sigma \mathbf{h}^\theta}{\mathcal{AB}(\theta)\Gamma(\theta+2)} \\ &\quad \times \sum_{\ell=1}^k \left[s_\ell^{\sigma-1} \mathbb{Q}_3(s_\ell, L_{1,\ell}, L_{2,\ell}, L_{3,\ell}) \hat{Y}_1(k, \ell) - s_{\ell-1}^{\sigma-1} \mathbb{Q}_3(s_{\ell-1}, L_{1,\ell-1}, L_{2,\ell-1}, L_{3,\ell-1}) \hat{Y}_2(k, \ell) \right], \end{aligned} \quad (35)$$

where

$$\hat{Y}_1(k, \ell) = (k+1-\ell)^\theta (k-\ell+2+\theta) - (k-\ell)^\theta (k-\ell+2+2\theta)$$

and

$$\hat{Y}_2(k, \ell) = (k+1-\ell)^{\theta+1} - (k-\ell)^\theta (k-\ell+1+\theta).$$

7 Numerical algorithm via Newton's polynomials

Here we develop a different approximation algorithm (based on Newton's Polynomials) to compute numerically the solutions of our fractal-fractional polluted lake system (4). The use of Newton's polynomials in interpolation is motivated by their simplicity and applicability for approximating functions based on a set of given data points. In the context of modeling and analysis, Newton's polynomials offer a flexible approach to represent complex relationships within the polluted lake system. The polynomial interpolation technique enables us to construct a continuous function that approximates the behavior of the system, facilitating a more detailed and comprehensive understanding of its dynamics. To the best of our knowledge, the idea was first introduced in [26]. Precisely, we follow [26] with the IVP (10) subject to the conditions (11) and (12). In this case, we have

$$\mathbb{K}(s) - \mathbb{K}(0) = \frac{\theta\sigma}{\mathcal{AB}(\theta)\Gamma(\theta)} \int_0^s \mathbf{w}^{\sigma-1} (s - \mathbf{w})^{\theta-1} \mathbb{Q}(\mathbf{w}, \mathbb{K}(\mathbf{w})) \, d\mathbf{w} + \frac{(1-\theta)\sigma s^{\sigma-1}}{\mathcal{AB}(\theta)} \mathbb{Q}(s, \mathbb{K}(s)).$$

Set $\mathbb{Q}^*(s, \mathbb{K}(s)) = \sigma s^{\sigma-1} \mathbb{Q}(s, \mathbb{K}(s))$. Then,

$$\mathbb{K}(s) - \mathbb{K}(0) = \frac{\theta}{\mathcal{AB}(\theta)\Gamma(\theta)} \int_0^s (s - \mathbf{w})^{\theta-1} \mathbb{Q}^*(\mathbf{w}, \mathbb{K}(\mathbf{w})) \, d\mathbf{w} + \frac{(1-\theta)}{\mathcal{AB}(\theta)} \mathbb{Q}^*(s, \mathbb{K}(s)).$$

By discretizing the above equation at $s = s_{k+1} = (k+1)\mathbf{h}$, we get

$$\mathbb{K}(s_{k+1}) - \mathbb{K}(0) = \frac{\theta}{\mathcal{AB}(\theta)\Gamma(\theta)} \int_0^{s_{k+1}} (s_{k+1} - \mathbf{w})^{\theta-1} \mathbb{Q}^*(\mathbf{w}, \mathbb{K}(\mathbf{w})) \, d\mathbf{w} + \frac{(1-\theta)}{\mathcal{AB}(\theta)} \mathbb{Q}^*(s_k, \mathbb{K}(s_k)).$$

Approximating the above integral, we can write that

$$\begin{aligned} \mathbb{K}(s_{k+1}) &= \mathbb{K}_0 + \frac{(1-\theta)}{\mathcal{AB}(\theta)} \mathbb{Q}^*(s_k, \mathbb{K}(s_k)) \\ &\quad + \frac{\theta}{\mathcal{AB}(\theta)\Gamma(\theta)} \sum_{\ell=2}^k \int_{s_\ell}^{s_{\ell+1}} (s_{k+1} - \mathbf{w})^{\theta-1} \mathbb{Q}^*(\mathbf{w}, \mathbb{K}(\mathbf{w})) \, d\mathbf{w}. \end{aligned} \quad (36)$$

Now we approximate function $\mathbb{Q}^*(s, \mathbb{K}(s))$ with the Newton polynomial

$$\begin{aligned} P_k^*(\mathbf{w}) &= \mathbb{Q}^*(s_{k-2}, \mathbb{K}(s_{k-2})) + \frac{\mathbb{Q}^*(s_{k-1}, \mathbb{K}(s_{k-1})) - \mathbb{Q}^*(s_{k-2}, \mathbb{K}(s_{k-2}))}{\mathbf{h}} (\mathbf{w} - s_{k-2}) \\ &\quad + \frac{\mathbb{Q}^*(s_k, \mathbb{K}(s_k)) - 2\mathbb{Q}^*(s_{k-1}, \mathbb{K}(s_{k-1})) + \mathbb{Q}^*(s_{k-2}, \mathbb{K}(s_{k-2}))}{2\mathbf{h}^2} (\mathbf{w} - s_{k-2})(\mathbf{w} - s_{k-1}). \end{aligned} \quad (37)$$

Substituting (37) into (36), we obtain that

$$\begin{aligned} \mathbb{K}_{k+1} &= \mathbb{K}_0 + \frac{(1-\theta)}{\mathcal{AB}(\theta)} \mathbb{Q}^*(s_k, \mathbb{K}(s_k)) + \frac{\theta}{\mathcal{AB}(\theta)\Gamma(\theta)} \sum_{\ell=2}^k \int_{s_\ell}^{s_{\ell+1}} \left[\mathbb{Q}^*(s_{\ell-2}, \mathbb{K}_{\ell-2}) \right. \\ &\quad + \frac{\mathbb{Q}^*(s_{\ell-1}, \mathbb{K}_{\ell-1}) - \mathbb{Q}^*(s_{\ell-2}, \mathbb{K}_{\ell-2})}{\mathbf{h}} (\mathbf{w} - s_{\ell-2}) \\ &\quad \left. + \frac{\mathbb{Q}^*(s_\ell, \mathbb{K}_\ell) - 2\mathbb{Q}^*(s_{\ell-1}, \mathbb{K}_{\ell-1}) + \mathbb{Q}^*(s_{\ell-2}, \mathbb{K}_{\ell-2})}{2\mathbf{h}^2} (\mathbf{w} - s_{\ell-2})(\mathbf{w} - s_{\ell-1}) \right] \\ &\quad \times (s_{k+1} - \mathbf{w})^{\theta-1} \, d\mathbf{w}. \end{aligned}$$

Simplifying the above relations, we get

$$\mathbb{K}_{k+1} = \mathbb{K}_0 + \frac{(1-\theta)}{\mathcal{AB}(\theta)} \mathbb{Q}^*(s_k, \mathbb{K}(s_k))$$

$$\begin{aligned}
 & + \frac{\theta}{\mathcal{AB}(\theta)\Gamma(\theta)} \sum_{\ell=2}^k \left[\int_{s_\ell}^{s_{\ell+1}} \mathbb{Q}^*(s_{\ell-2}, \mathbb{K}_{\ell-2})(s_{k+1} - \mathfrak{w})^{\theta-1} d\mathfrak{w} \right. \\
 & + \int_{s_\ell}^{s_{\ell+1}} \frac{\mathbb{Q}^*(s_{\ell-1}, \mathbb{K}_{\ell-1}) - \mathbb{Q}^*(s_{\ell-2}, \mathbb{K}_{\ell-2})}{\mathbf{h}} (\mathfrak{w} - s_{\ell-2})(s_{k+1} - \mathfrak{w})^{\theta-1} d\mathfrak{w} \\
 & + \int_{s_\ell}^{s_{\ell+1}} \frac{\mathbb{Q}^*(s_\ell, \mathbb{K}_\ell) - 2\mathbb{Q}^*(s_{\ell-1}, \mathbb{K}_{\ell-1}) + \mathbb{Q}^*(s_{\ell-2}, \mathbb{K}_{\ell-2})}{2\mathbf{h}^2} (\mathfrak{w} - s_{\ell-2})(\mathfrak{w} - s_{\ell-1}) \\
 & \left. \times (s_{k+1} - \mathfrak{w})^{\theta-1} d\mathfrak{w} \right]
 \end{aligned}$$

and it follows that

$$\begin{aligned}
 \mathbb{K}_{k+1} & = \mathbb{K}_0 + \frac{(1-\theta)}{\mathcal{AB}(\theta)} \mathbb{Q}^*(s_k, \mathbb{K}(s_k)) \\
 & + \frac{\theta}{\mathcal{AB}(\theta)\Gamma(\theta)} \sum_{\ell=2}^k \mathbb{Q}^*(s_{\ell-2}, \mathbb{K}_{\ell-2}) \int_{s_\ell}^{s_{\ell+1}} (s_{k+1} - \mathfrak{w})^{\theta-1} d\mathfrak{w} \\
 & + \frac{\theta}{\mathcal{AB}(\theta)\Gamma(\theta)} \sum_{\ell=2}^k \frac{\mathbb{Q}^*(s_{\ell-1}, \mathbb{K}_{\ell-1}) - \mathbb{Q}^*(s_{\ell-2}, \mathbb{K}_{\ell-2})}{\mathbf{h}} \int_{s_\ell}^{s_{\ell+1}} (\mathfrak{w} - s_{\ell-2})(s_{k+1} - \mathfrak{w})^{\theta-1} d\mathfrak{w} \\
 & + \frac{\theta}{\mathcal{AB}(\theta)\Gamma(\theta)} \sum_{\ell=2}^k \frac{\mathbb{Q}^*(s_\ell, \mathbb{K}_\ell) - 2\mathbb{Q}^*(s_{\ell-1}, \mathbb{K}_{\ell-1}) + \mathbb{Q}^*(s_{\ell-2}, \mathbb{K}_{\ell-2})}{2\mathbf{h}^2} \\
 & \times \int_{s_\ell}^{s_{\ell+1}} (\mathfrak{w} - s_{\ell-2})(\mathfrak{w} - s_{\ell-1})(s_{k+1} - \mathfrak{w})^{\theta-1} d\mathfrak{w}.
 \end{aligned} \tag{38}$$

On the other hand, by computing the above three integrals separately, one gets

$$\int_{s_\ell}^{s_{\ell+1}} (s_{k+1} - \mathfrak{w})^{\theta-1} d\mathfrak{w} = \frac{\mathbf{h}^\theta}{\theta} [(k-\ell+1)^\theta - (k-\ell)^\theta], \tag{39}$$

$$\begin{aligned}
 & \int_{s_\ell}^{s_{\ell+1}} (\mathfrak{w} - s_{\ell-2})(s_{k+1} - \mathfrak{w})^{\theta-1} d\mathfrak{w} \\
 & = \frac{\mathbf{h}^{\theta+1}}{\theta(\theta+1)} [(k-\ell+1)^\theta(k-\ell+3+2\theta) - (k-\ell+1)^\theta(k-\ell+3+3\theta)], \tag{40}
 \end{aligned}$$

and

$$\begin{aligned}
 & \int_{s_\ell}^{s_{\ell+1}} (\mathfrak{w} - s_{\ell-2})(\mathfrak{w} - s_{\ell-1})(s_{k+1} - \mathfrak{w})^{\theta-1} d\mathfrak{w} = \frac{\mathbf{h}^{\theta+2}}{\theta(\theta+1)(\theta+2)} \left((k-\ell+1)^\theta [2(k-\ell)^2 \right. \\
 & \quad + (3\theta+10)(k-\ell) + 2\theta^2 + 9\theta + 12] - (k-\ell)^\theta [2(k-\ell)^2 \\
 & \quad \left. + (5\theta+10)(k-\ell) + 6\theta^2 + 18\theta + 12] \right). \tag{41}
 \end{aligned}$$

By putting (39), (40), and (41) into (38), we obtain that

$$\mathbb{K}_{k+1} = \mathbb{K}_0 + \frac{(1-\theta)}{\mathcal{AB}(\theta)} \mathbb{Q}^*(s_k, \mathbb{K}(s_k))$$

$$\begin{aligned}
 & + \frac{\theta \mathbf{h}^\theta}{\mathcal{AB}(\theta)\Gamma(\theta+1)} \sum_{\ell=2}^k \mathbb{Q}^*(s_{\ell-2}, \mathbb{K}_{\ell-2}) [(k-\ell+1)^\theta - (k-\ell)^\theta] \\
 & + \frac{\theta \mathbf{h}^\theta}{\mathcal{AB}(\theta)\Gamma(\theta+2)} \sum_{\ell=2}^k [\mathbb{Q}^*(s_{\ell-1}, \mathbb{K}_{\ell-1}) - \mathbb{Q}^*(s_{\ell-2}, \mathbb{K}_{\ell-2})] \\
 & \times [(k-\ell+1)^\theta (k-\ell+3+2\theta) - (k-\ell+1)^\theta (k-\ell+3+3\theta)] \\
 & + \frac{\theta \mathbf{h}^\theta}{2\mathcal{AB}(\theta)\Gamma(\theta+3)} \sum_{\ell=2}^k [\mathbb{Q}^*(s_\ell, \mathbb{K}_\ell) - 2\mathbb{Q}^*(s_{\ell-1}, \mathbb{K}_{\ell-1}) + \mathbb{Q}^*(s_{\ell-2}, \mathbb{K}_{\ell-2})] \\
 & \times [(k-\ell+1)^\theta [2(k-\ell)^2 + (3\theta+10)(k-\ell) + 2\theta^2 + 9\theta + 12] - (k-\ell)^\theta [2(k-\ell)^2 \\
 & + (5\theta+10)(k-\ell) + 6\theta^2 + 18\theta + 12]]. \tag{42}
 \end{aligned}$$

Finally, we replace $\mathbb{Q}^*(s, \mathbb{K}(s)) = \sigma s^{\sigma-1} \mathbb{Q}(s, \mathbb{K}(s))$ into (42), and we get that

$$\begin{aligned}
 \mathbb{K}_{k+1} & = \mathbb{K}_0 + \frac{(1-\theta)\sigma s_k^{\sigma-1}}{\mathcal{AB}(\theta)} \mathbb{Q}(s_k, \mathbb{K}(s_k)) \\
 & + \frac{\theta \sigma \mathbf{h}^\theta}{\mathcal{AB}(\theta)\Gamma(\theta+1)} \sum_{\ell=2}^k s_{\ell-2}^{\sigma-1} \mathbb{Q}(s_{\ell-2}, \mathbb{K}_{\ell-2}) \hat{\Psi}_1(k, \ell, \theta) \\
 & + \frac{\theta \sigma \mathbf{h}^\theta}{\mathcal{AB}(\theta)\Gamma(\theta+2)} \sum_{\ell=2}^k [s_{\ell-1}^{\sigma-1} \mathbb{Q}(s_{\ell-1}, \mathbb{K}_{\ell-1}) - s_{\ell-2}^{\sigma-1} \mathbb{Q}(s_{\ell-2}, \mathbb{K}_{\ell-2})] \hat{\Psi}_2(k, \ell, \theta) \\
 & + \frac{\theta \sigma \mathbf{h}^\theta}{2\mathcal{AB}(\theta)\Gamma(\theta+3)} \sum_{\ell=2}^k [s_\ell^{\sigma-1} \mathbb{Q}(s_\ell, \mathbb{K}_\ell) - 2s_{\ell-1}^{\sigma-1} \mathbb{Q}(s_{\ell-1}, \mathbb{K}_{\ell-1}) + s_{\ell-2}^{\sigma-1} \mathbb{Q}(s_{\ell-2}, \mathbb{K}_{\ell-2})] \hat{\Psi}_3(k, \ell, \theta), \tag{43}
 \end{aligned}$$

where

$$\begin{aligned}
 \hat{\Psi}_1(k, \ell, \theta) & = (k-\ell+1)^\theta - (k-\ell)^\theta, \\
 \hat{\Psi}_2(k, \ell, \theta) & = (k-\ell+1)^\theta (k-\ell+3+2\theta) - (k-\ell)^\theta (k-\ell+3+3\theta), \\
 \hat{\Psi}_3(k, \ell, \theta) & = (k-\ell+1)^\theta [2(k-\ell)^2 + (3\theta+10)(k-\ell) + 2\theta^2 + 9\theta + 12] \\
 & \quad - (k-\ell)^\theta [2(k-\ell)^2 + (5\theta+10)(k-\ell) + 6\theta^2 + 18\theta + 12]. \tag{44}
 \end{aligned}$$

Using the numerical scheme (43), the numerical solutions to the fractal-fractional polluted lake system (4) are given by

$$\begin{aligned}
 L_{1,k+1} &= L_{1,0} + \frac{(1-\theta)\sigma s_k^{\sigma-1}}{\mathcal{AB}(\theta)} \mathbb{Q}_1(s_k, L_1(s_k), L_2(s_k), L_3(s_k)) \\
 &+ \frac{\theta\sigma\mathbf{h}^\theta}{\mathcal{AB}(\theta)\Gamma(\theta+1)} \sum_{\ell=2}^k s_{\ell-2}^{\sigma-1} \mathbb{Q}_1(s_{\ell-2}, L_{1,\ell-2}, L_{2,\ell-2}, L_{3,\ell-2}) \hat{\Psi}_1(k, \ell, \theta) \\
 &+ \frac{\theta\sigma\mathbf{h}^\theta}{\mathcal{AB}(\theta)\Gamma(\theta+2)} \sum_{\ell=2}^k \left[s_{\ell-1}^{\sigma-1} \mathbb{Q}_1(s_{\ell-1}, L_{1,\ell-1}, L_{2,\ell-1}, L_{3,\ell-1}) \right. \\
 &\quad \left. - s_{\ell-2}^{\sigma-1} \mathbb{Q}_1(s_{\ell-2}, L_{1,\ell-2}, L_{2,\ell-2}, L_{3,\ell-2}) \right] \hat{\Psi}_2(k, \ell, \theta) \\
 &+ \frac{\theta\sigma\mathbf{h}^\theta}{2\mathcal{AB}(\theta)\Gamma(\theta+3)} \sum_{\ell=2}^k \left[s_{\ell}^{\sigma-1} \mathbb{Q}_1(s_{\ell}, L_{1,\ell}, L_{2,\ell}, L_{3,\ell}) \right. \\
 &\quad \left. - 2s_{\ell-1}^{\sigma-1} \mathbb{Q}_1(s_{\ell-1}, L_{1,\ell-1}, L_{2,\ell-1}, L_{3,\ell-1}) \right. \\
 &\quad \left. + s_{\ell-2}^{\sigma-1} \mathbb{Q}_1(s_{\ell-2}, L_{1,\ell-2}, L_{2,\ell-2}, L_{3,\ell-2}) \right] \hat{\Psi}_3(k, \ell, \theta),
 \end{aligned} \tag{45}$$

$$\begin{aligned}
 L_{2,k+1} &= L_{2,0} + \frac{(1-\theta)\sigma s_k^{\sigma-1}}{\mathcal{AB}(\theta)} \mathbb{Q}_2(s_k, L_1(s_k), L_2(s_k), L_3(s_k)) \\
 &+ \frac{\theta\sigma\mathbf{h}^\theta}{\mathcal{AB}(\theta)\Gamma(\theta+1)} \sum_{\ell=2}^k s_{\ell-2}^{\sigma-1} \mathbb{Q}_2(s_{\ell-2}, L_{1,\ell-2}, L_{2,\ell-2}, L_{3,\ell-2}) \hat{\Psi}_1(k, \ell, \theta) \\
 &+ \frac{\theta\sigma\mathbf{h}^\theta}{\mathcal{AB}(\theta)\Gamma(\theta+2)} \sum_{\ell=2}^k \left[s_{\ell-1}^{\sigma-1} \mathbb{Q}_2(s_{\ell-1}, L_{1,\ell-1}, L_{2,\ell-1}, L_{3,\ell-1}) \right. \\
 &\quad \left. - s_{\ell-2}^{\sigma-1} \mathbb{Q}_2(s_{\ell-2}, L_{1,\ell-2}, L_{2,\ell-2}, L_{3,\ell-2}) \right] \hat{\Psi}_2(k, \ell, \theta) \\
 &+ \frac{\theta\sigma\mathbf{h}^\theta}{2\mathcal{AB}(\theta)\Gamma(\theta+3)} \sum_{\ell=2}^k \left[s_{\ell}^{\sigma-1} \mathbb{Q}_2(s_{\ell}, L_{1,\ell}, L_{2,\ell}, L_{3,\ell}) \right. \\
 &\quad \left. - 2s_{\ell-1}^{\sigma-1} \mathbb{Q}_2(s_{\ell-1}, L_{1,\ell-1}, L_{2,\ell-1}, L_{3,\ell-1}) \right. \\
 &\quad \left. + s_{\ell-2}^{\sigma-1} \mathbb{Q}_2(s_{\ell-2}, L_{1,\ell-2}, L_{2,\ell-2}, L_{3,\ell-2}) \right] \hat{\Psi}_3(k, \ell, \theta),
 \end{aligned} \tag{46}$$

and

$$\begin{aligned}
 L_{3,k+1} &= L_{3,0} + \frac{(1-\theta)\sigma s_k^{\sigma-1}}{\mathcal{AB}(\theta)} \mathbb{Q}_3(s_k, L_1(s_k), L_2(s_k), L_3(s_k)) \\
 &+ \frac{\theta\sigma\mathbf{h}^\theta}{\mathcal{AB}(\theta)\Gamma(\theta+1)} \sum_{\ell=2}^k s_{\ell-2}^{\sigma-1} \mathbb{Q}_3(s_{\ell-2}, L_{1,\ell-2}, L_{2,\ell-2}, L_{3,\ell-2}) \hat{\Psi}_1(k, \ell, \theta) \\
 &+ \frac{\theta\sigma\mathbf{h}^\theta}{\mathcal{AB}(\theta)\Gamma(\theta+2)} \sum_{\ell=2}^k \left[s_{\ell-1}^{\sigma-1} \mathbb{Q}_3(s_{\ell-1}, L_{1,\ell-1}, L_{2,\ell-1}, L_{3,\ell-1}) \right. \\
 &\left. - s_{\ell-2}^{\sigma-1} \mathbb{Q}_3(s_{\ell-2}, L_{1,\ell-2}, L_{2,\ell-2}, L_{3,\ell-2}) \right] \hat{\Psi}_2(k, \ell, \theta) \\
 &+ \frac{\theta\sigma\mathbf{h}^\theta}{2\mathcal{AB}(\theta)\Gamma(\theta+3)} \sum_{\ell=2}^k \left[s_\ell^{\sigma-1} \mathbb{Q}_3(s_\ell, L_{1,\ell}, L_{2,\ell}, L_{3,\ell}) \right. \\
 &\left. - 2s_{\ell-1}^{\sigma-1} \mathbb{Q}_3(s_{\ell-1}, L_{1,\ell-1}, L_{2,\ell-1}, L_{3,\ell-1}) \right. \\
 &\left. + s_{\ell-2}^{\sigma-1} \mathbb{Q}_3(s_{\ell-2}, L_{1,\ell-2}, L_{2,\ell-2}, L_{3,\ell-2}) \right] \hat{\Psi}_3(k, \ell, \theta),
 \end{aligned} \tag{47}$$

where $\hat{\Psi}_j(k, \ell, \theta)$ are defined in (44), $j = 1, 2, 3$.

8 Numerical simulations and discussion

Now we apply the Adams–Bashforth method (ABM) and Newton’s polynomials method (NPM), proposed respectively in Sections 6 and 7, to examine and find numerical solutions L_1, L_2, L_3 of the proposed FF-model and to observe the applicability, accuracy, and exactness of the developed algorithms. To simulate the quantity of pollution in the modeled lakes, we coded the algorithms (33)–(35) and (45)–(47) in MATLAB, version R2019A.

To compare the results, we borrow from [1] the following values for the parameters: $F_{21} = 18 \text{ mi}^3/\text{year}$, $F_{31} = 20 \text{ mi}^3/\text{year}$, $F_{32} = 18 \text{ mi}^3/\text{year}$, $F_{13} = 38 \text{ mi}^3/\text{year}$, $V_1 = 2900 \text{ mi}^3$, $V_2 = 850 \text{ mi}^3$, $V_3 = 1180 \text{ mi}^3$. Moreover, $L_{1,0} = L_{2,0} = L_{3,0} = 0$. Also, various fractal dimensions and fractional orders, i.e., $\theta = \sigma = 0.85, 0.90, 0.95, 0.99$, are considered for the simulations of the three state functions L_1, L_2 , and L_3 .

We consider the suggested FF-model in three cases: linear (Section 8.1), exponentially decaying (Section 8.2), and periodic (Section 8.3) input models.

8.1 Linear input model

In this case, we consider the model in which the Lake 1 has a contaminant with a linear concentration. Linear input states the steady behavior of the pollutant. At time zero, the pollutant concentration is zero but, as the time increases, the addition of pollutant is started and then is remained steadily. For example, when a factory starts production at time zero, waste discharge begins at a fixed rate and concentration. As a particular case, we chose $c(s) = \mu s$. Then, for $\mu = 100$, from (4) we have

$$\begin{cases}
 \text{FFML} \mathcal{D}_{0,s}^{(\theta,\sigma)} L_1(s) = \frac{38}{1180} L_3(s) + 100s - \frac{20}{2900} L_1(s) - \frac{18}{2900} L_1(s), \\
 \text{FFML} \mathcal{D}_{0,s}^{(\theta,\sigma)} L_2(s) = \frac{18}{2900} L_1(s) - \frac{18}{850} L_2(s), \\
 \text{FFML} \mathcal{D}_{0,s}^{(\theta,\sigma)} L_3(s) = \frac{20}{2900} L_1(s) + \frac{18}{850} L_2(s) - \frac{38}{1180} L_3(s).
 \end{cases} \tag{48}$$

In Figures 2 (a), (b), and (c), the behavior of the ABM approximations for each pair of the state functions $L_1 - L_2$, $L_1 - L_3$, and $L_2 - L_3$, respectively, are given; while in Figure 2 (d), the 3D

view of $L_1 - L_2 - L_3$ under integer-order derivatives are graphically illustrated for the linear input model with time $s \in [0, 60]$ and step size $h = 0.1$.

Note that the parameter h is explicitly defined as the step size, distinct from the stability parameters h_j , $j \in \{1, 2, 3\}$, discussed in the stability Section 5. While here we emphasize h as the step size in a specific context, Ulam–Hyers–Rassias stability, as a theory, is primarily concerned with the stability properties of functional equations. Unlike the numerical solution of differential equations, the choice of step size is not a direct consideration in the realm of Ulam–Hyers–Rassias stability. This stability theory focuses on understanding how small variations in functional equations lead to proportionate changes in the solutions, and the concept of a step size does not play a prominent role in that context.

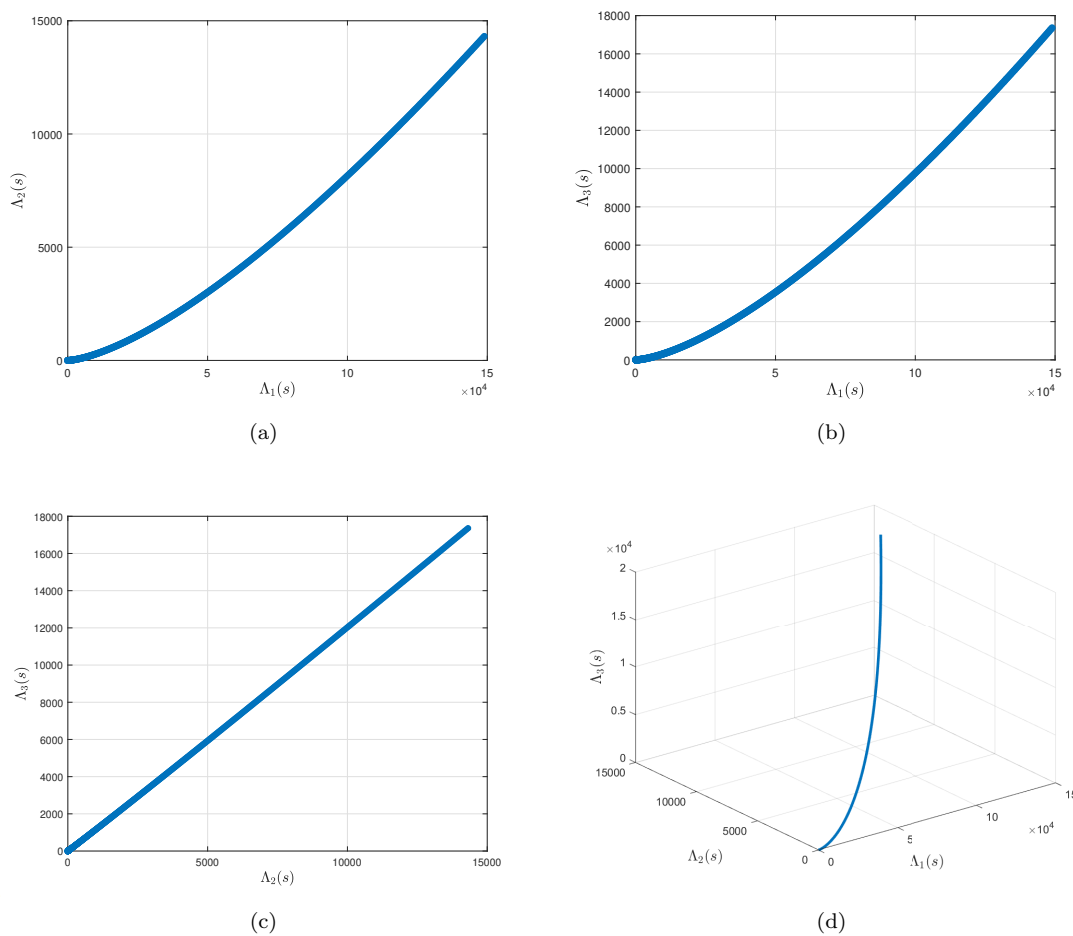


Figure 2: Behaviors of each pair of state functions (a) $L_1 - L_2$, (b) $L_1 - L_3$, (c) $L_2 - L_3$ and (d) 3D view of $L_1 - L_2 - L_3$ under the integer-order.

In Table 1, we present some numerical results of the two numerical techniques, ABM and NPM, for the three state functions L_1 , L_2 and L_3 in the linear input case, under integer-order derivatives and step size $h = 0.1$. From the obtained numerical results, we can assert that the Adams–Bashforth approximations for the phase functions L_1 , L_2 , and L_3 strongly agree with the ones obtained by the Newton polynomials method for the time s up to 10 years.

In Figure 3, the comparison of the numerical results from ABM and NPM for the state functions L_1 , L_2 , and L_3 is shown graphically, for the time $s \in [0, 60]$ and the linear input case. We observe that the results of ABM and NPM have a high agreement between them for each one of the state

Table 1: Comparison between ABM and NPM for the linear input case.

s	Adams–Bashforth			Newton Polynomials		
	L_1	L_2	L_3	L_1	L_2	L_3
0	0.000000	0.000000	0.000000	0.000000	0.000000	0.000000
1	58.241762	0.122200	0.136038	58.249029	0.114027	0.126944
2	216.569135	0.912690	1.018175	216.603012	0.891958	0.995030
3	472.231987	2.959673	3.308340	472.291839	2.926723	3.271438
4	824.018631	6.830863	7.650506	824.103833	6.786029	7.600138
5	1270.753481	13.074750	14.671769	1270.863423	13.018359	14.608218
6	1811.296055	22.221220	24.982726	1811.430139	22.153588	24.906273
7	2444.539990	34.782156	39.177854	2444.697632	34.703595	39.088774
8	3169.412094	51.252025	57.835881	3169.592721	51.162836	57.734443
9	3984.871413	72.108440	81.520147	3985.074465	72.008917	81.406618
10	4889.908324	97.812711	110.778966	4890.133254	97.703141	110.653605

functions, even in the longer period of 60 years.

In Figure 4, we illustrate the behavior of the three state functions L_1 , L_2 , and L_3 when the ABM is applied under the fractal-fractional orders $\theta = \sigma = 0.85, 0.90, 0.95, 0.99$. From these figures, we can observe that when the fractal-fractional order is getting closer to the integer case, then the effect of the pollution is increasing on each lake model at about the same rate. As an observation of these graphs, it can be said that the non-integer order operator has a positive effect on the pollution reduction in the lake pollution model.

A word is due about our choice of the values of the fractal-fractional orders. We considered fractional orders within the range of $[0.85, 1]$ because within this interval we observed consistent behaviors for different fractional orders. Specifically, as the fractal-fractional order decreases, we noted a proportional reduction in the impact of pollution on each lake model at about the same rate. This consistent trend in behavior as the fractional order decreases led us to cut the interval at the value 0.85. This choice captures the essential aspects of the model’s response to varying fractional orders and provides a meaningful representation of the system dynamics.

8.2 Exponentially decaying input model

When heavy dumping of pollutant is present, it makes sense to consider the exponentially decaying input model, i.e., the case when $c(s) = re^{-ps}$. An example of this case occurs if every industry placed in a city collects and stores its wastage during some days and then dumps it to Lake 1 after that stored period. If we take $r = 200$ and $p = 10$, then system (4) becomes

$$\begin{cases} \text{FFML}\mathcal{D}_{0,s}^{(\theta,\sigma)} L_1(s) = \frac{38}{1180} L_3(s) + 200e^{-10s} - \frac{20}{2900} L_1(s) - \frac{18}{2900} L_1(s), \\ \text{FFML}\mathcal{D}_{0,s}^{(\theta,\sigma)} L_2(s) = \frac{18}{2900} L_1(s) - \frac{18}{850} L_2(s), \\ \text{FFML}\mathcal{D}_{0,s}^{(\theta,\sigma)} L_3(s) = \frac{20}{2900} L_1(s) + \frac{18}{850} L_2(s) - \frac{38}{1180} L_3(s). \end{cases} \quad (49)$$

The graphical representation of the input function $c(s)$ is illustrated in Figure 5 for the exponentially decaying input case $c(s) = 200e^{-10s}$, $s \in [0, 1]$.

In Figures 6 (a), (b), and (c), the behavior of the ABM approximations for each pair of the state functions $L_1 - L_2$, $L_1 - L_3$, and $L_2 - L_3$, respectively, is shown, while in Figure 6 (d), the 3D view of $L_1 - L_2 - L_3$ under the integer-order derivative is graphically illustrated for the exponentially decaying input model with time $s \in [0, 60]$ and step size $h = 0.01$.

In Table 2, we provide a comparison between the approximate solutions obtained using ABM and NPM for the exponentially decaying input case with time $s \in [0, 10]$, step size $h = 0.01$,

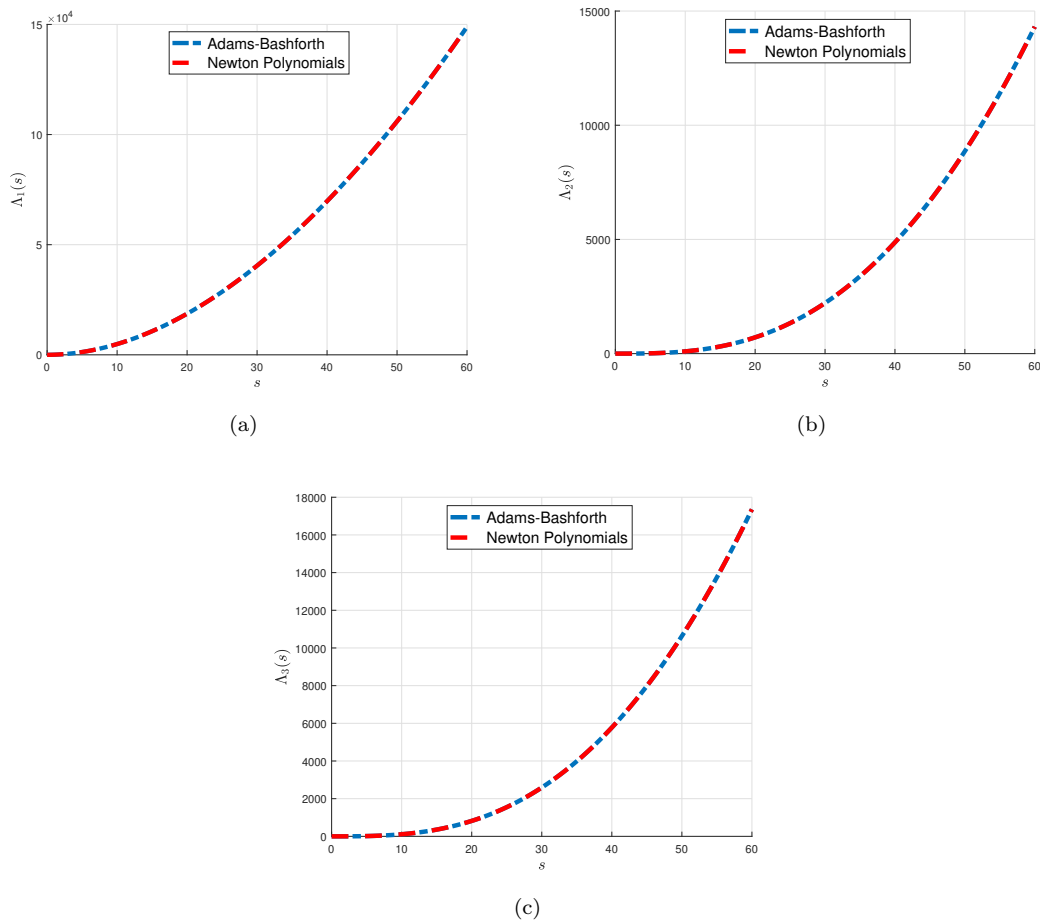


Figure 3: Comparison between the ABM and NPM for (a) $L_1(s)$, (b) $L_2(s)$ and (c) $L_3(s)$ in the linear input model.

and $\theta = \sigma = 1$. From Table 2, we can conclude that the ABM approximations are also in good agreement with the NPM ones for the exponentially decaying input model.

In Figure 7, we present a graphical comparison between ABM and NPM approximations for the state functions L_1 , L_2 , and L_3 in the exponentially decaying input case with time $s \in [0, 60]$. From Figure 7, it can be concluded that the two introduced methods strongly agree with each other even in a large time domain of 60 years.

In Figure 8, we illustrate the numerical results of the three state variables L_1, L_2 , and L_3 for the exponentially decaying input model when the ABM is applied under various fractal-fractional orders: $\theta = \sigma = 0.85, 0.90, 0.95, 0.99$. Figure 8 shows that the non-integer fractal-fractional operators have an effect on decreasing the amount of pollution for each model when the time s increases, that is, the pollution is increasing harmoniously with the fractal-fractional order, getting closer to the integer-order case.

8.3 Periodic input model

As a last case of study, we consider a periodic input model in which the pollutant appears in the lake periodically. A factory that works during daytime only, can be an example of this case: it generates waste and dump it in the lakes during the day while at night the mixing of new pollutants stops. For a concrete case, we selected $c(s) = a + \tau \sin(bs)$, where τ and b stands for

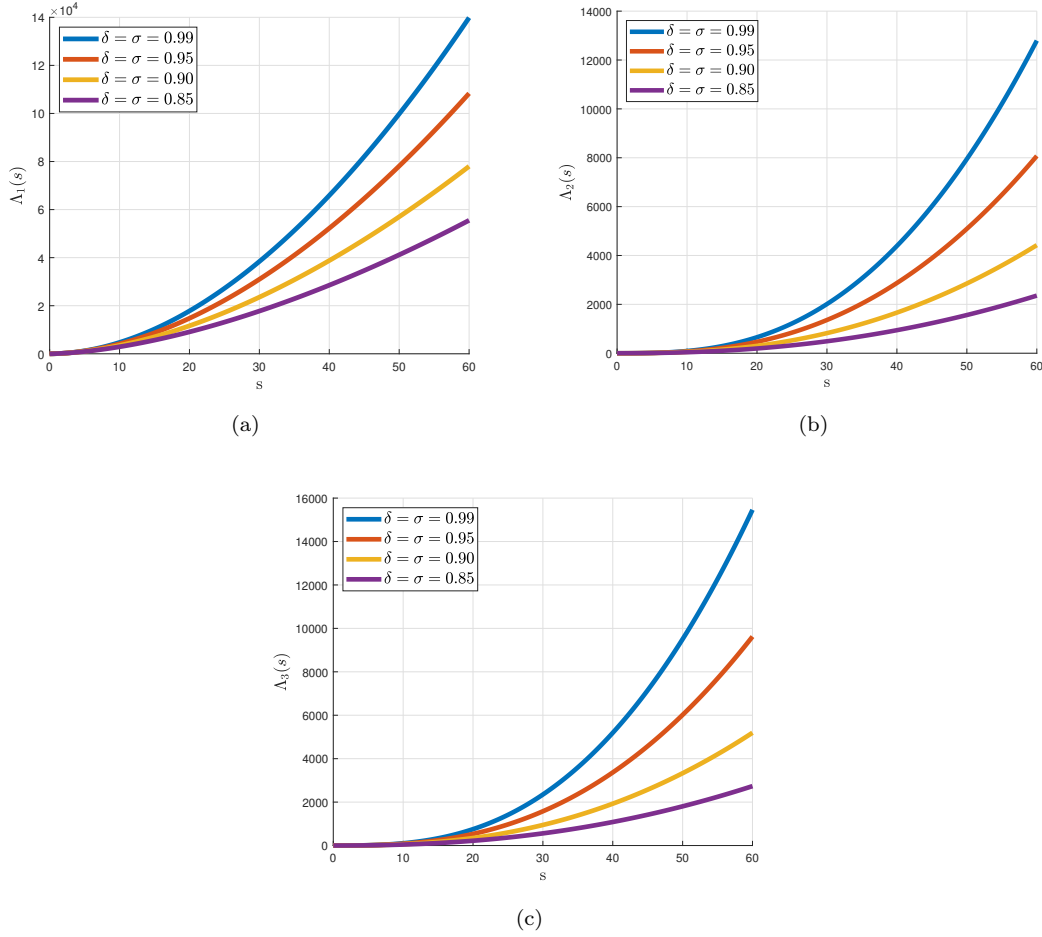


Figure 4: Behaviors of (a) $L_1(s)$, (b) $L_2(s)$ and (c) $L_3(s)$ for the linear input model under fractal and fractional orders $\theta = \sigma = 0.85, 0.90, 0.95, 0.99$.

the variations of amplitude and frequency, respectively. Also, a is considered as the average input of pollutant concentration. In such a case $a = b = \tau = 1$, system (4) takes the following form:

$$\begin{cases} \mathbf{FFML}\mathcal{D}_{0,s}^{(\theta,\sigma)} L_1(s) = \frac{38}{1180} L_3(s) + 1 + \sin(s) - \frac{20}{2900} L_1(s) - \frac{18}{2900} L_1(s), \\ \mathbf{FFML}\mathcal{D}_{0,s}^{(\theta,\sigma)} L_2(s) = \frac{18}{2900} L_1(s) - \frac{18}{850} L_2(s), \\ \mathbf{FFML}\mathcal{D}_{0,s}^{(\theta,\sigma)} L_3(s) = \frac{20}{2900} L_1(s) + \frac{18}{850} L_2(s) - \frac{38}{1180} L_3(s). \end{cases} \quad (50)$$

The graphical representation of the input function $c(s)$ is illustrated in Figure 9 for the periodic input case $c(s) = 1 + \sin(s)$, $s \in [0, 20]$.

In Figures 10 (a), (b), and (c), the graphical behavior of each pair of the state functions $L_1 - L_2$, $L_1 - L_3$, and $L_2 - L_3$, respectively, is shown. In Figure 10 (d), the 3D view of $L_1 - L_2 - L_3$ under the integer-order derivative is illustrated for the periodic input model with time $s \in [0, 60]$ and step size $h = 0.1$.

The tabular comparison between the numerical results obtained from the proposed techniques, ABM and NPM, for the three state functions L_1 , L_2 , and L_3 under the periodic input case, are reported in Table 3 for time $s \in [0, 10]$, step size $h = 0.1$, and $\theta = \sigma = 1$. From these results, we conclude that the solutions obtained by ABM and NPM highly agree with each other.

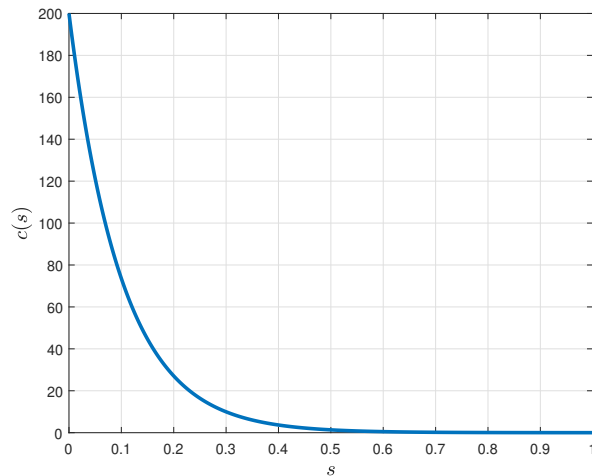


Figure 5: Graphic of the exponentially decaying input.

Table 2: Numerical comparison between ABM and NPM for the exponentially decaying input case.

s	Adams–Bashforth			Newton Polynomials		
	L_1	L_2	L_3	L_1	L_2	L_3
0	0.000000	0.000000	0.000000	0.000000	0.000000	0.000000
1	18.988642	0.105437	0.117578	18.988592	0.105145	0.117021
2	18.748146	0.219107	0.245295	18.752821	0.216590	0.242237
3	18.513934	0.328934	0.369679	18.523194	0.324269	0.364185
4	18.286698	0.435044	0.490805	18.300406	0.428303	0.482940
5	18.066244	0.537556	0.608748	18.084267	0.528808	0.598573
6	17.852383	0.636586	0.723579	17.874593	0.625901	0.711155
7	17.644931	0.732247	0.835369	17.671201	0.719691	0.820757
8	17.443709	0.824649	0.944190	17.473918	0.810285	0.927446
9	17.248540	0.913898	1.050109	17.282570	0.897787	1.031291
10	17.059256	1.000097	1.153195	17.096990	0.982299	1.132359

In Figure 11, we illustrate our findings graphically, comparing the numerical results from ABM and NPM for each state function L_1 , L_2 , and L_3 , where the Lake 1 has a periodic pollutant input. Figure 11 shows that the two introduced techniques, ABM and NPM, strongly agree with each other for the time $s \in [0, 60]$, step size $h = 0.1$, and $\theta = \sigma = 1$.

In Figure 12, we illustrate the ABM approximations of the three state functions L_1 , L_2 , and L_3 under various fractal-fractional orders: $\theta = \sigma = 0.85, 0.90, 0.95, 0.99$ for the periodic input case. Similar to cases of Sections 8.1 and 8.2, we observe that the non-integer order fractal-fractional operators have a great effect on decreasing the amount of contamination for each model while the time s increases.

9 Conclusion

We employed Mittag–Leffler type kernels to solve a system of fractional differential equations using fractal-fractional (FF) operators with two fractal and fractional orders. We derived equiv-

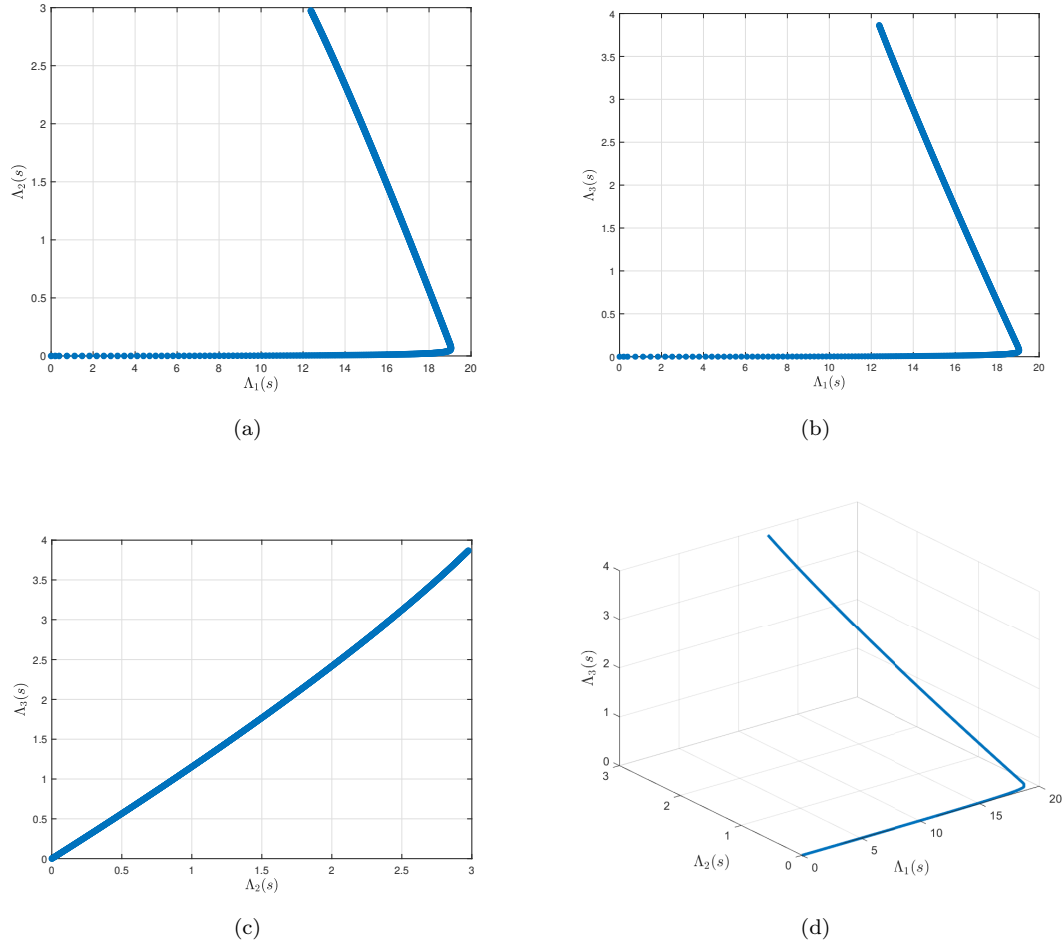


Figure 6: Behaviors of each pair of state functions (a) $L_1 - L_2$, (b) $L_1 - L_3$, (c) $L_2 - L_3$ and (d) 3D view of $L_1 - L_2 - L_3$ under the integer-order.

Table 3: Comparison between ABM and NPM in the periodic input case.

s	Adams–Bashforth			Newton Polynomials		
	L_1	L_2	L_3	L_1	L_2	L_3
0	0.000000	0.000000	0.000000	0.000000	0.000000	0.000000
1	1.420794	0.003639	0.004053	1.420289	0.003637	0.004052
2	3.352256	0.018270	0.020396	3.349409	0.017505	0.019538
3	4.795526	0.043383	0.048562	4.791798	0.041836	0.046821
4	5.304589	0.073971	0.083050	5.303706	0.071660	0.080440
5	5.281611	0.104988	0.118274	5.286096	0.101974	0.114856
6	5.607511	0.135825	0.153543	5.616323	0.132176	0.149388
7	6.832362	0.170701	0.193553	6.841809	0.166454	0.188698
8	8.669954	0.214629	0.243923	8.677051	0.209775	0.238353
9	10.261233	0.268650	0.305891	10.266407	0.263162	0.299573
10	10.964396	0.328730	0.375035	10.971053	0.322611	0.367966

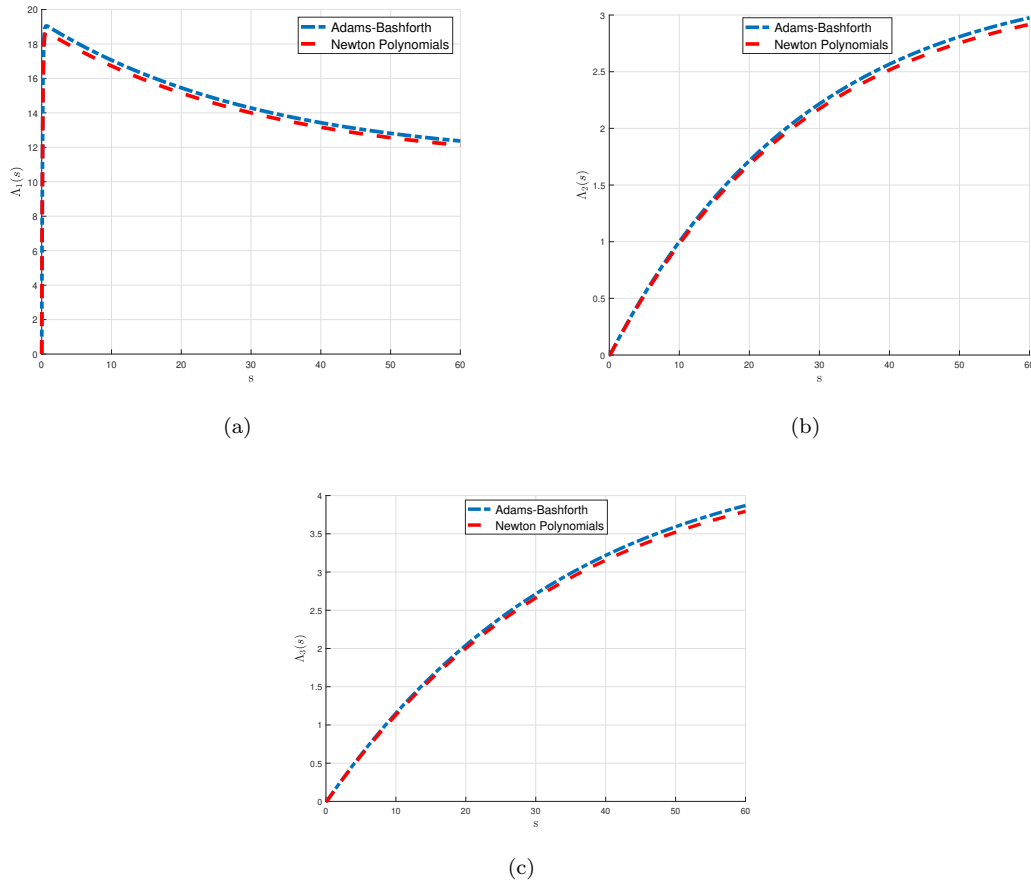


Figure 7: Comparison between the ABM and NPM for (a) $L_1(s)$, (b) $L_2(s)$ and (c) L_3 in the exponentially decaying input model.

alent FF-integral equations from a compact initial value problem, and then proved existence and uniqueness results. A stability analysis was conducted in different versions. In the next sections, we examined and captured the behavior of the considered fractal-fractional operator model (4) with the help of two different numerical techniques: an Adams–Bashforth method (ABM) and a Newton polynomials method (NPM). From the obtained results, we conclude that the considered techniques, ABM and NPM, are in highly agreement and are very efficient to examine the system of fractional differential equations under fractal-fractional operators describing the dynamics of the pollution in the lakes. We also analyzed the considered model under various fractal-fractional orders and examined the effects of these non-integer orders on the behavior of each state variable $L_1(s)$, $L_2(s)$, and $L_3(s)$ for three specific input models: linear, exponentially decaying, and periodic. For each input model, we observed that when the fractal-fractional order gets closer to the classical integer-order case, then the effect of the pollution is increasing harmoniously for each lake model. As a conclusion of these observations, it can be said that the non-integer order operators have positive effects on the reduction of pollution in the lake pollution model. As future work, we plan to investigate different real-world models based on the techniques here developed.

CRedit authorship contribution statement

Tanzeela Kanwal: Formal analysis, Methodology. **Azhar Hussain:** Conceptualization, Formal analysis, Methodology. **İbrahim Avci:** Formal analysis, Methodology, Software. **Sina Etemad:**

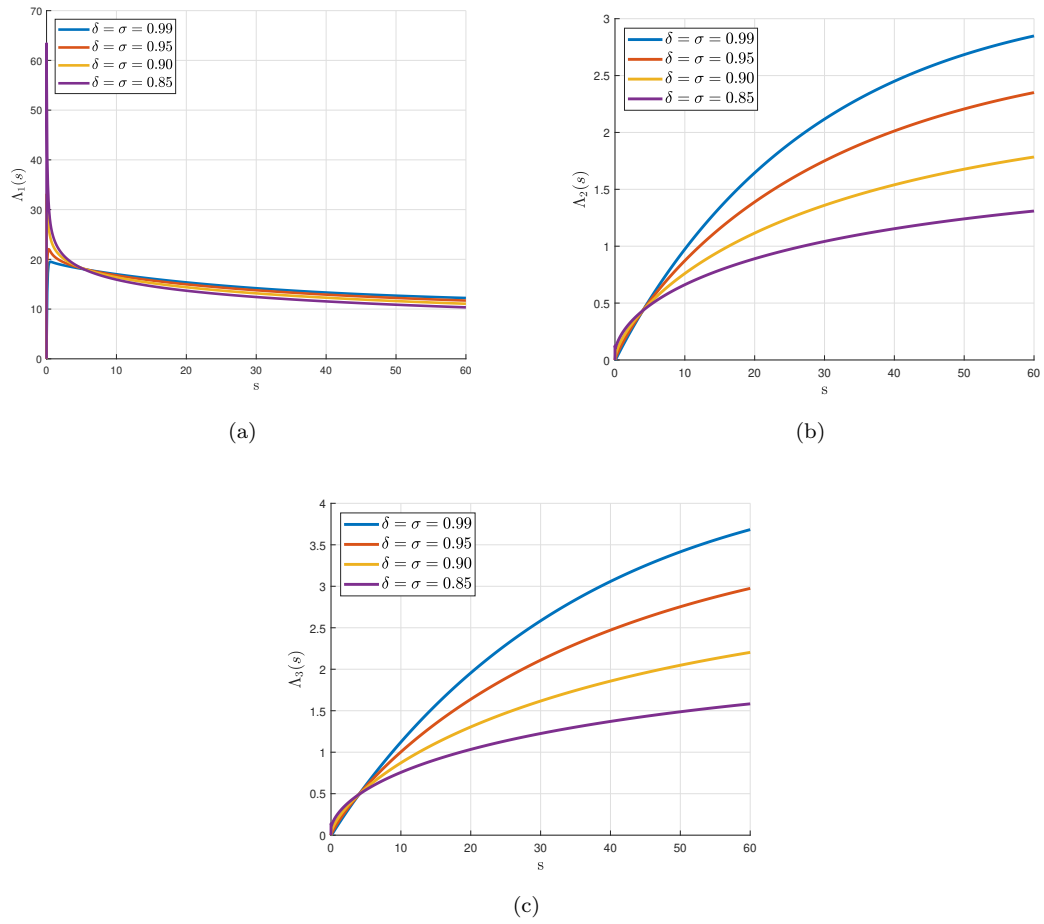


Figure 8: Behaviors of (a) $L_1(s)$, (b) $L_2(s)$ and (c) $L_3(s)$ for the exponentially decaying input model under fractal and fractional orders $\theta = \sigma = 0.85, 0.90, 0.95, 0.99$.

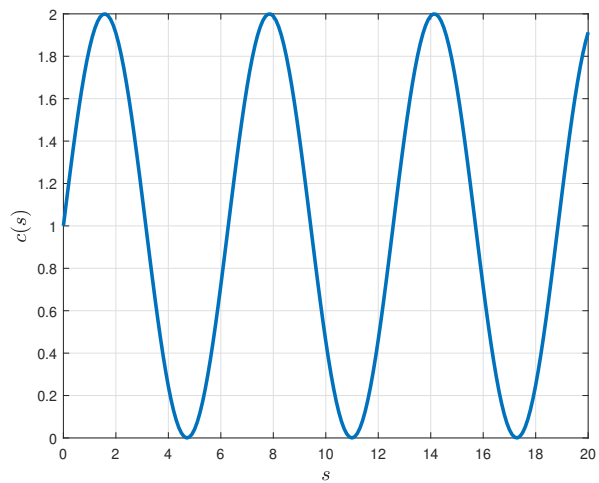


Figure 9: Graphic of the periodic input.

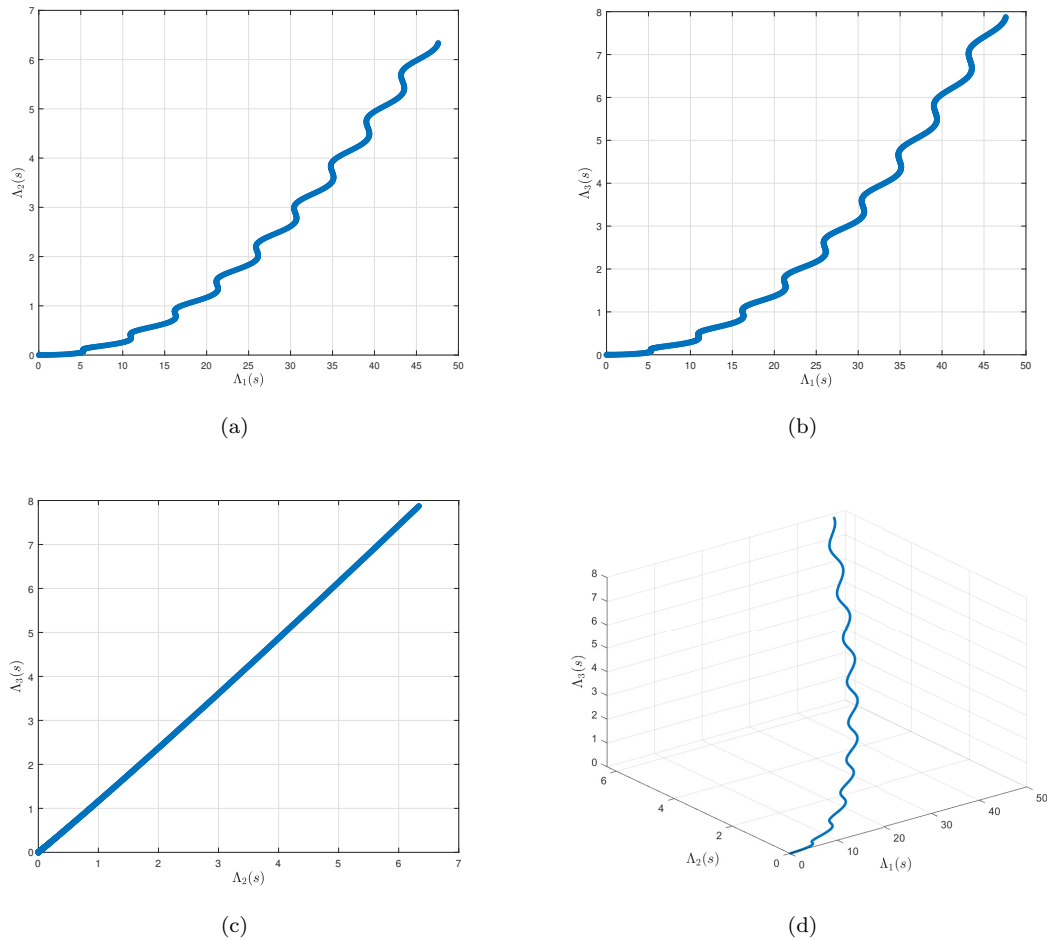


Figure 10: Behaviors of each pair of state functions (a) $L_1 - L_2$, (b) $L_1 - L_3$, (c) $L_2 - L_3$ and (d) 3D view of $L_1 - L_2 - L_3$ under the integer-order.

Conceptualization, Methodology, Software. **Shahram Rezapour:** Conceptualization, Methodology. **Delfim F. M. Torres:** Formal analysis, Funding acquisition, Methodology.

Declaration of competing interest

The authors declare that they have no known competing financial interests or personal relationships that could have appeared to influence the work reported in this paper.

Data availability

No data was used for the research described in the article.

Acknowledgments

Torres was supported by the Portuguese Foundation for Science and Technology (FCT), project UIDB/04106/2020 (<https://doi.org/10.54499/UIDB/04106/2020>).

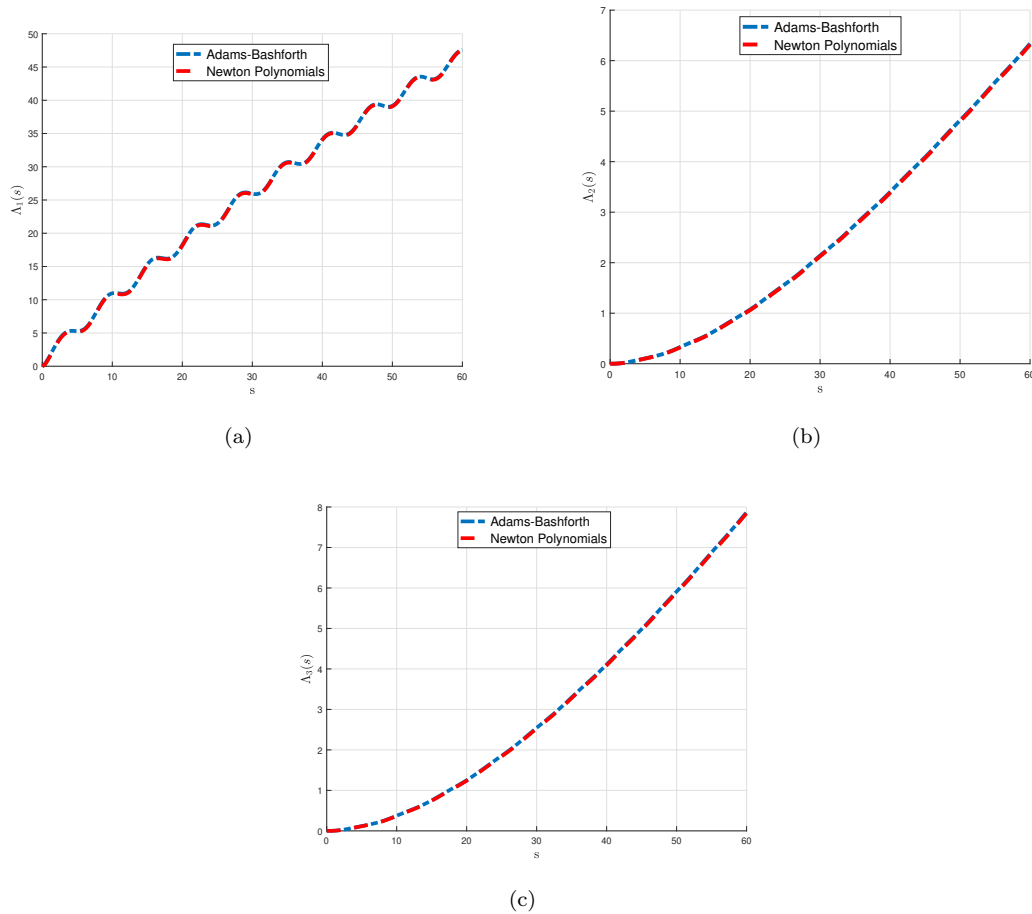


Figure 11: Comparison between the ABM and NPM for (a) $L_1(s)$, (b) $L_2(s)$ and (c) L_3 in the periodic input model.

References

- [1] J. Biazar, L. Farrokhi, M. R. Islam, Modeling the pollution of a system of lakes. *Appl. Math. Comput.*, **178**(2) (2006) 423–430. <https://doi.org/10.1016/j.amc.2005.11.056>
- [2] Ş. Yüzbaşı, N. Şahin, M. Sezer, A collocation approach to solving the model of pollution for a system of lakes, *Math. Computer Model.*, **55**(3-4) (2012) 330–341. <https://doi.org/10.1016/j.mcm.2011.08.007>
- [3] B. Benhammouda, H. Vazquez-Leal, L. Hernandez-Martinez, Modified differential transform method for solving the model of pollution for a system of lakes, *Discr. Dyn. Nat. Soc.*, **2014** (2014) 645726. <https://doi.org/10.1155/2014/645726>
- [4] M. M. Khader, T. S. El Danaf, A. S. Hendy, A computational matrix method for solving systems of high order fractional differential equations, *Appl. Math. Model.*, **37**(6) (2013) 4035–4050. <https://doi.org/10.1016/j.apm.2012.08.009>
- [5] N. Bildik, S. Deniz, A new fractional analysis on the polluted lakes system, *Chaos, Solitons & Fractals*, **122** (2019) 17–24. <https://doi.org/10.1016/j.chaos.2019.02.001>
- [6] M. M. D. Ahmed, M. A. Khan, Modeling and analysis of the polluted lakes system with various fractional approaches, *Chaos, Solitons & Fractals*, **134** (2020) 109720. <https://doi.org/10.1016/j.chaos.2020.109720>
- [7] D. G. Prakasha, P. Veerasha, Analysis of Lakes pollution model with Mittag-Leffler kernel, *J. Ocean Eng. Sci.*, **5**(4) (2020) 310–322. <https://doi.org/10.1016/j.joes.2020.01.004>

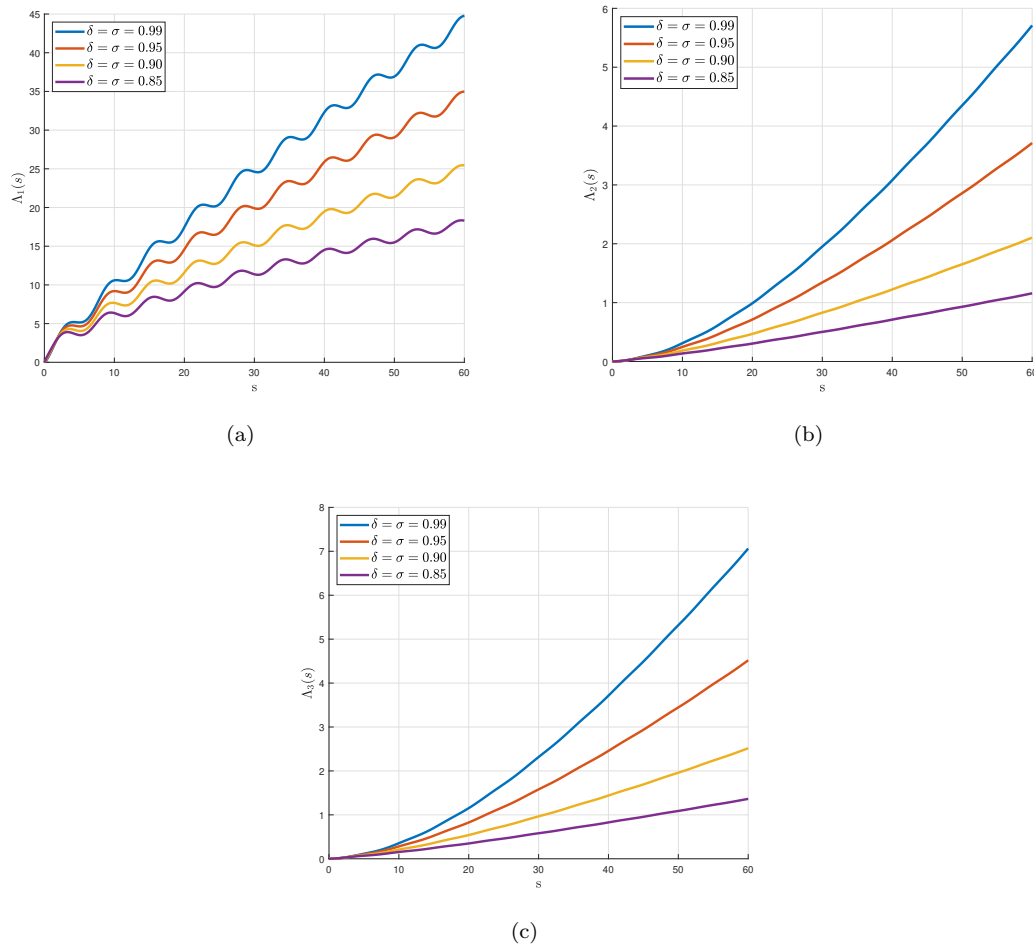


Figure 12: Behaviors of (a) $L_1(s)$, (b) $L_2(s)$ and (c) $L_3(s)$ for the periodic input model under fractal and fractional orders $\theta = \sigma = 0.85, 0.90, 0.95, 0.99$.

- [8] B. Shiri, D. Baleanu, A General Fractional Pollution Model for Lakes, *Commun. Appl. Math. Comput.*, **4** (2022) 1105–1130. <https://doi.org/10.1007/s42967-021-00135-4>
- [9] A. Alsaedi, M. Alsulami, H. M. Srivastava, B. Ahmad, S. K. Ntouyas, Existence theory for nonlinear third-order ordinary differential equations with nonlocal multi-point and multi-strip boundary conditions, *Symmetry*, **11**(2) (2019) 281. <https://doi.org/10.3390/sym11020281>
- [10] M. R. Sidi Ammi, M. Tahiri, D. F. M. Torres, Necessary optimality conditions of a reaction-diffusion SIR model with ABC fractional derivatives, *Discrete Contin. Dyn. Syst. Ser. S* **15** (2022), no. 3, 621–637. <https://doi.org/10.3934/dcdss.2021155> [arXiv:2106.15055](https://arxiv.org/abs/2106.15055)
- [11] M. Aslam, R. Murtaza, T. Abdeljawad, G. ur Rahman, A. Khan, H. Khan, H. Gulzar, A fractional order HIV/AIDS epidemic model with Mittag-Leffler kernel, *Adv. Differ. Equ.*, **2021** (2021), 107, 1–5. <https://doi.org/10.1186/s13662-021-03264-5>
- [12] S. W. Ahmad, M. Sarwar, G. Rahmat, K. Shah, H. Ahmad, A. A. A. Mousa, Fractional order model for the Coronavirus (COVID-19) in Wuhan, China, *Fractals*, **30** (2022), 2240007. <https://doi.org/10.1142/S0218348X22400072>
- [13] J. K. K. Asamoah, E. Okyere, E. Yankson, A. A. Opoku, A. Adom-Konadu, E. Acheampong, Y. D. Arthur, Non-fractional and fractional mathematical analysis and simulations for Q fever, *Chaos, Solitons & Fractals*, **156** (2022), 111821. <https://doi.org/10.1016/j.chaos.2022.111821>

- [14] H. Khan, Y. G. Li, W. Chen, D. Baleanu, A. Khan, Existence theorems and Hyers-Ulam stability for a coupled system of fractional differential equations with p -Laplacian operator, *Bound. Value Probl.*, **2017** (2017), 157, 1–16. <https://doi.org/10.1186/s13661-017-0878-6>
- [15] Z. Ali, F. Rabiei and K. Hosseini, A fractal-fractional-order modified Predator-Prey mathematical model with immigrations, *Math. Comput. Simulation* **207** (2023), 466–481. <https://doi.org/10.1016/j.matcom.2023.01.006>
- [16] A. Atangana, Fractal-fractional differentiation and integration: connecting fractal calculus and fractional calculus to predict complex system, *Chaos, Solitons & Fractals*, **102** (2017) 396–406. <https://doi.org/10.1016/j.chaos.2017.04.027>
- [17] K. Shah, M. Arfan, I. Mahariq, A. Ahmadian, S. Salahshour, M. Ferrara, Fractal-fractional mathematical model addressing the situation of Corona virus in Pakistan, *Res. Phys.*, **19** (2020) 103560. <https://doi.org/10.1016/j.rinp.2020.103560>
- [18] J. F. Gomez-Aguilar, T. Cordova-Fraga, T. Abdeljawad, A. Khan, H. Khan, Analysis of fractal-fractional Malaria transmission model, *Fractals*, **28**(08) (2020) 2040041. <https://doi.org/10.1142/S0218348X20400411>
- [19] Z. Ali, F. Rabiei, K. Shah, T. Khodadadi, Qualitative analysis of fractal-fractional order COVID-19 mathematical model with case study of Wuhan, *Alex. Eng. J.*, **60**(1) (2021) 477–489. <https://doi.org/10.1016/j.aej.2020.09.020>
- [20] S. Etemad, I. Avci, P. Kumar, D. Baleanu, S. Rezapour, Some novel mathematical analysis on the fractal-fractional model of the AH1N1/09 virus and its generalized Caputo-type version, *Chaos, Solitons & Fractals*, **162** (2022) 112511. <https://doi.org/10.1016/j.chaos.2022.112511>
- [21] J. K. K. Asamoah, Fractal-fractional model and numerical scheme based on Newton polynomial for Q fever disease under Atangana-Baleanu derivative, *Res. Phys.*, **34** (2022) 105189. <https://doi.org/10.1016/j.rinp.2022.105189>
- [22] S. Ahmad, A. Ullah, A. Akgul, M. De la Sen, Study of HIV disease and its association with immune cells under nonsingular and nonlocal fractal-fractional operator, *Complexity*, **2021** (2021) 1904067. <https://doi.org/10.1155/2021/1904067>
- [23] H. Najafi, S. Etemad, N. Patanarapeelert, J. K. K. Asamoah, S. Rezapour, T. Sitthiwirattham, A study on dynamics of CD4⁺ T-cells under the effect of HIV-1 infection based on a mathematical fractal-fractional model via the Adams-Bashforth scheme and Newton polynomials, *Mathematics*, **10** (2022) 1366. <https://doi.org/10.3390/math10091366>
- [24] H. Khan, K. Alam, H. Gulzar, S. Etemad, S. Rezapour, A case study of fractal-fractional tuberculosis model in China: Existence and stability theories along with numerical simulations, *Math. Comput. Simul.*, **198** (2022) 455–473. <https://doi.org/10.1016/j.matcom.2022.03.009>
- [25] A. Granas, J. Dugundji, *Fixed Point Theory*, Springer-Verlag, New York (2003).
- [26] A. Atangana, S. İ Araz, *New numerical scheme with Newton polynomial—theory, methods, and applications*, Elsevier/Academic Press, London, 2021.